ORNL-3609
UC-34 – Physics
TID-4500 (34th ed.)

PULSE-HEIGHT SPECTRA OF GAMMA RAYS EMITTED BY THE STAINLESS-STEEL-CLAD BULK SHIELDING REACTOR II (BSR-II)

G. T. Chapman
K. M. Henry
J. D. Jarrard

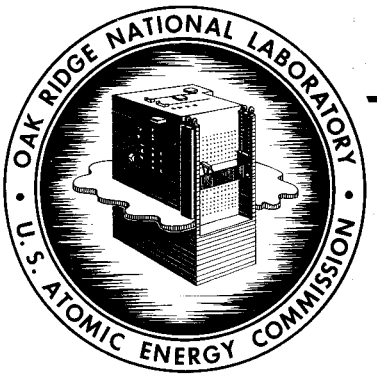

OAK RIDGE NATIONAL LABORATORY
operated by
UNION CARBIDE CORPORATION
for the
U.S. ATOMIC ENERGY COMMISSION

Printed in USA. Price $3.00. Available from the Clearinghouse for Federal Scientific and Technical Information, National Bureau of Standards, U.S. Department of Commerce, Springfield, Virginia

ORNL-3609

Contract No. W-7405-eng-26

Neutron Physics Division

PULSE-HEIGHT SPECTRA OF GAMMA RAYS EMITTED BY THE STAINLESS-STEEL-CLAD BULK SHIELDING REACTOR II (BSR-II)

G. T. Chapman, K. M. Henry, and J. D. Jarrard

NOVEMBER 1964

OAK RIDGE NATIONAL LABORATORY
Oak Ridge, Tennessee
operated by
UNION CARBIDE CORPORATION
for the
U. S. ATOMIC ENERGY COMMISSION

TABLE OF CONTENTS

PULSE-HEIGHT SPECTRA OF GAMMA RAYS EMITTED BY THE STAINLESS-STEEL-CLAD BULK SHIELDING REACTOR II (BSR-II)

G. T. Chapman, K. M. Henry, and J. D. Jarrard[1]

ABSTRACT

Measurements have been made of the pulse-height spectra of gamma rays emitted from the core of the Bulk Shielding Reactor II (BSR-II). Preliminary analysis of the data indicates that the gamma rays having energies above 5 MeV originate primarily from thermal-neutron capture in the stainless steel reactor structure. Below 5 MeV the spectrum is apparently composed of the expected continua of prompt-fission and fission-product gamma rays plus a large contribution from thermal-neutron captures in the hydrogen of the water that moderates and reflects the core. Except for reduced intensity, little change was noticed in the structure of the distribution as the amount of water between the reactor surface and the spectrometer was increased from 1 to 60 cm. Angular-distribution measurements were also made about two points at 10 and 25 cm from the surface of the reactor. A simple calculation of the expected spectra at the surface of a homogeneous reactor compared favorably with a measured spectrum.

INTRODUCTION

Measurements of the pulse-height spectra of gamma rays emitted from the water-moderated and -reflected stainless-steel-clad core of the Bulk Shielding Reactor II (BSR-II)[2] have been made with the Model IV gamma-ray spectrometer, a total-absorption NaI(Tl) spectrometer developed at the Bulk Shielding Facility especially for these measurements. The reactor configuration consisted of a simple 5 x 4 array of "cold"[3] BSR-II fuel

---

[1]Present address: Technical Operations Research, Fort Monroe, Va.

[2]E. G. Silver and J. Lewin, Safeguard Report for a Stainless-Steel Reactor for the BSF (BSR-II), ORNL-2470 (July 16, 1958).

elements loaded in the Pool Critical Assembly[4] (PCA). This particular loading reduced the number of core-scattered gamma rays and thus made the results more readily comparable with simple calculations.

Spectra were also obtained with increasing thicknesses of water between the reactor surface and the spectrometer to provide data for an experimental check on the attenuation theories currently in use or which may be originated for shield design and studies. Two additional sets of data were taken with the spectrometer rotated about points in the water at 10 and 25 cm, respectively, from the reactor surface to study the angular distributions of the gamma rays at these points.

The data are presented as pulse-height spectra rather than energy spectra since the effects of imperfect instrument response have not been removed. A preliminary examination indicates, however, that most of the predominant structure of the distributions is readily identifiable with expected gamma rays resulting from the capture of thermal neutrons in the components of the reactor material.

THE MODEL IV GAMMA-RAY SPECTROMETER

A cutaway drawing of the Model IV gamma-ray spectrometer as used in this study is shown in Fig. 1. Basically, it consisted of a large NaI(Tl) crystal encased in a 15-ton shield which had an air-filled collimator extending from one end. The shield material consisted of a lead-lithium

---

[3] "Cold" elements are those which have been used only during low-power reactor operations and thus have not suffered any considerable amount of fission-product buildup.

[4] E. B. Johnson, Standard Operating Procedure for the Pool Critical Assembly, ORNL-2449 (Aug. 12, 1960).

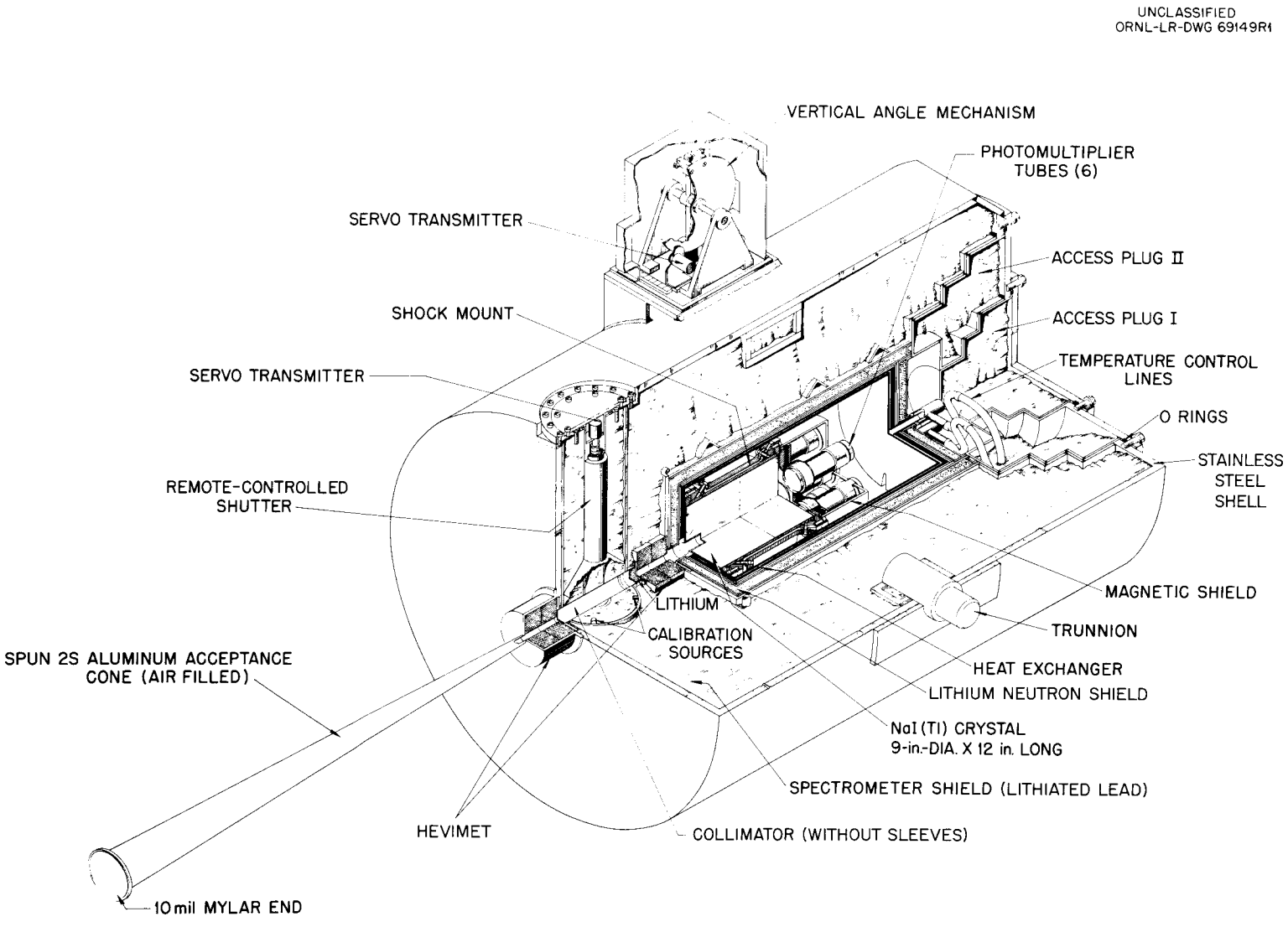

Fig. 1. The Model IV Gamma-Ray Spectrometer.

eutectic (0.62 wt % natural lithium) whose thickness was 14 in. at the front, 12 in. at the side, and 10 in. at the back. The entire spectrometer was contained in a water-tight stainless steel shell. All instrument cables were brought into the back of the shield through 180° spiral holes in a large access plug (plug II), which prevented there being a straight path for radiation through the shield. Additional neutron shielding was provided inside the shield by a 1-in.-thick layer of lithium contained in a thin stainless steel shell completely surrounding a heat exchanger, which contained the NaI(Tl) crystal. The heat exchanger was thermally insulated from the internal neutron shield.

Located in the wall at the front of the shield was a remotely operated shutter composed of the same lead-lithium eutectic as the shield wall. A servomechanism arrangement made it possible to position the shutter either to open a collimator hole for allowing external radiation to reach the crystal or to close the hole for making background measurements. In the closed position 6 in. of the lead alloy was introduced into the radiation path. The collimator hole through the shutter was 2 in. in diameter but by the insertion of lead sleeves could be reduced to the diameter that was desired. In this study a diameter of 1.14 cm was used.

Four small sources of gamma rays with known energies were embedded in the shutter material and could be individually positioned near the NaI(Tl) crystal for checking the electronic gain of the system at any time during operation. Immediately behind the shutter toward the interior of the shield was positioned a 1-in.-thick plug of lithium in the collimation hole to prevent thermal neutrons from reaching the crystal.

During the measurements reported here a collimator-acceptance cone system was used to define the solid angle for the acceptance of gamma rays

and to reduce the number of capture gamma rays produced in the material of the shield. The collimator (see Fig. 1) was 37.14 cm long, including 2 in. of high-density Hevimet (~90 wt % W, 6 wt % Ni, and 4 wt % Cu; density, 17 g/cm^3) placed at each end. Two more inches of Hevimet containing conical holes (half angle, 1° 47') were added to the original Hevimet at each end to reduce the amount of radiation penetrating the collimator edges. These pieces did not increase the collimator length since the half angle of each hole was equal to the half angle of the collimator-acceptance cone. The 4-in.-thick Hevimet at the crystal end of the collimation hole also helped to confine the gamma-ray beam more closely to the geometrical dimensions of the collimator.

The acceptance cone, which was constructed of spun 2S aluminum, was 54 in. long, had a diameter of 4.25 in. at the large end, was tapered to 0.574 in. at the shield, and had a half angle of 2.0°. The air void thus created was large enough to include the collimator solid angle and long enough to permit the approximately 55 in. of water shielding between the spectrometer shield and the reactor that had previously been indicated[5] as necessary. A 10-mil-thick Mylar window covered the large end of the cone.

NaI(Tl) Crystal

The NaI(Tl) detector is a composite formed by joining a 7-in.-long crystal to one that is 5 in. long, which results in a right-cylinder configuration that is 9 in. in diameter and 12 in. long. An optically consistent compound is used to connect the two crystals. The crystal is contained in the heat exchanger and is supported in a shock-mount-designed

---

[5]G. T. Chapman, Neutron Phys. Div. Ann. Progr. Rept. Sept. 1, 1961, ORNL-3193, p 197.

ring so as to be coaxial with the shield through $\pm 70^{\circ}$ vertical rotation and to be protected from sudden shock while the spectrometer is being moved.

Six 3-in.-diam photomultiplier tubes (6363) are also contained inside the heat exchanger and are mounted in a magnetic shield to protect them from stray electromagnetic fields and to assure that they are kept firmly pressed against the light windows in the crystal housing. Opthalmologically pure petroleum jelly is used as an optical coupling between the tubes and the glass of the light windows. The temperature of the tubes and the crystal, which is kept constant at $75 \pm 0.25^{\circ}$F, is measured by three iron-constantan thermocouples. The temperature control system consists of electrical heating coils and a Hilsch tube[6] for cooling and is mounted in the rear of the spectrometer shield.

The NaI(Tl) crystal is used to convert gamma-ray energy into light pulses, which are subsequently detected and amplified by the array of six photomultiplier tubes. The collimated gamma-ray beam was introduced into the crystal through a 1-in.-diam 2-in.-deep well drilled axially in one end. Monte Carlo[7,8] calculations had indicated that such a well would improve the response of the crystal by reducing the amount of energy lost as a result of scattered gamma rays escaping through the front surface of the crystal. A typical response curve obtained by collimating gamma rays into the crystal

---

[6] W. G. Stone and T. A. Love, An Experimental Study of the Hilsch Tube and Its Possible Application to Isotopic Separation, ORNL-282 (Jan. 4, 1950).

[7] C. D. Zerby and H. S. Moran, Neutron Phys. Div. Ann. Progr. Rept. Sept. 1, 1959, ORNL-2842, p 185.

[8] R. W. Peelle et al., Neutron Phys. Div. Ann. Progr. Rept. Sept. 1, 1959, ORNL-2842, p 187.

well is shown in Fig. 2. The measured pulse-height distribution shown is for gamma rays resulting from the decay of ^{16}N in the neutron-induced activity of demineralized water. It is easy to discern the 2.73-, 6.13-, and 7.12-MeV gamma rays in the ^{16}N decay. Contamination in the distribution is evident in the peak at 0.511 MeV, which results from an annihilation gamma ray originating in the lead, and the peak at 1.36 MeV, which is caused by a gamma ray resulting from the decay of ^{19}O. It will be noticed, however, that there is no evidence of escape peaks which might be associated with the 6.13-MeV gamma ray. The first such escape peak, at about 5.62 MeV (channel 87 in the figure), may have been "smeared" into the total-absorption peak by the resolution, but even so it still is not significant.

The measured resolution for the crystal as a function of energy is shown in Fig. 3. It has been assumed that the percent resolution of NaI(Tl) could be described by the negative one-half power of the gamma-ray energy, since this resolution had been observed[9] with smaller crystals mounted on single photomultiplier tubes; consequently it was somewhat unexpected to find that a least-squares fit to the data shown in Fig. 3 indicated that, for this crystal and photomultiplier tube array, the resolution is more closely represented by $E^{-0.344}$ over the energy range from 0.3 to 10 MeV. This indicates that further studies of the resolution function for an array of photomultiplier tubes on one crystal might prove useful.

Positioner

The device for transporting and positioning the 15-ton shield and spectrometer is shown in Fig. 4. Basically, it consists of a 20-ton mobile crane to provide the horizontal motion, a telescoping boom for vertical

---

[9] C. E. Crouthamel, Applied Gamma-Ray Spectroscopy, p 31, Pergamon, New York, 1960.

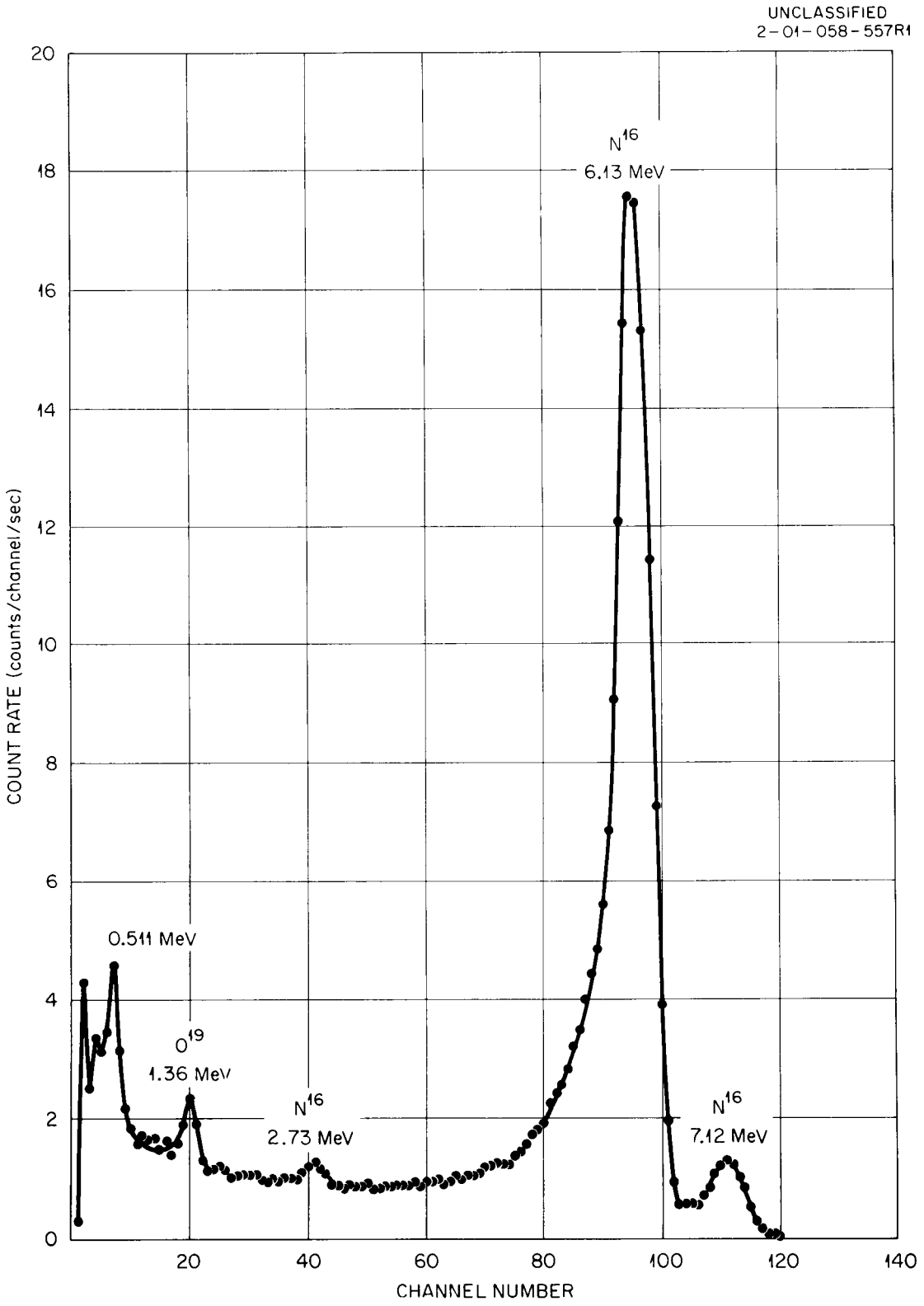

Fig. 2. Measured Response of the Model IV Gamma-Ray Spectrometer to 6.13-MeV Gamma Rays.

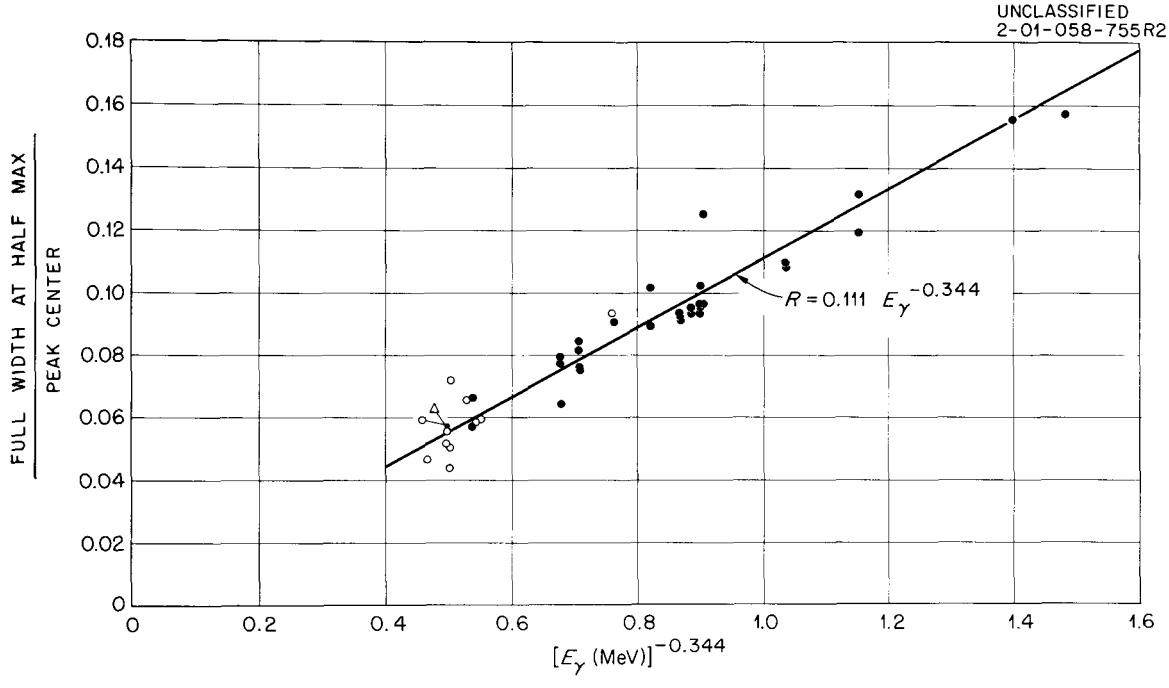

Fig. 3. The Measured Relative Resolution of the Model IV Gamma-Ray Spectrometer as a Function of Gamma-Ray Energy (E_γ).

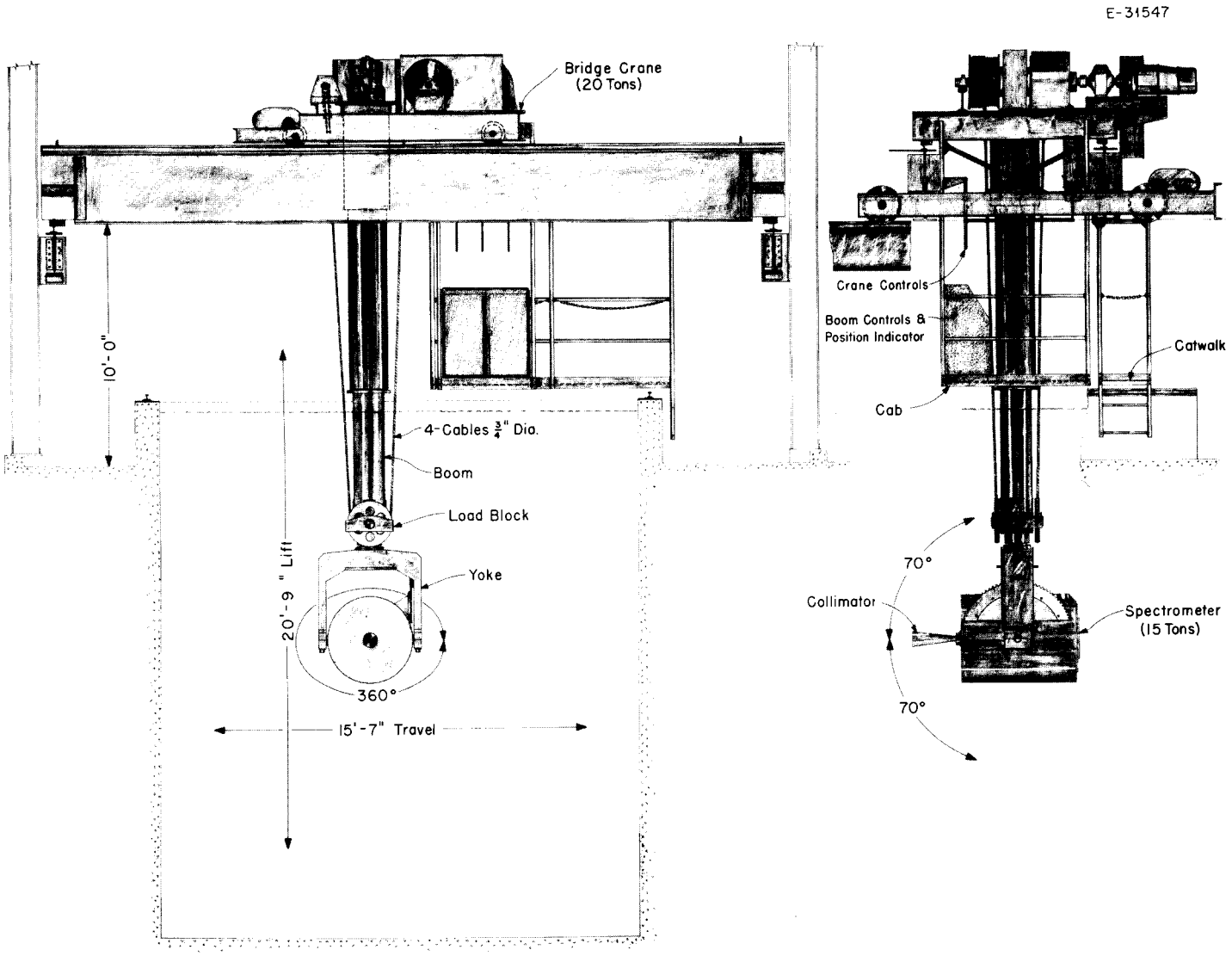

Fig. 4. Positioning Device for Model IV Gamma-Ray Spectrometer.

motion, a yoke for mounting the shield, and a simple analog computer for calculating[10] and reading out the position of the center point on the end of the acceptance cone. This system was designed to position the spectrometer at any point in the reactor pool relative to the front surface of the reactor within an accuracy of at least 0.7 cm in any linear coordinate reading. Each time a measurement was made, however, the position of the end of the cone was checked by means of a plumb-bob reading on an external scale independent of the read-out system. Since it was known that the spectrometer would have to be rotated through various horizontal angles, the reproducibility of the angle indicator was checked against points in the floor of the reactor-pool room that had previously been accurately determined by surveying instruments and methods. It was found that an angular measurement in a horizontal plane could be repeated within $\pm 0.23^{\circ}$.

Reactor Loading and Monitor System

The 5 x 4 array (Fig. 5) of stainless steel fuel elements that was used for loading the PCA resulted in an active core measuring 15 in. high by 15 in. wide by 12 in. deep, which was sufficient to maintain a critical assembly with simple geometry. This thin-core volume reduced the effects of core-scattered gamma rays on the measured spectra. A typical loading in the PCA position in the reactor pool is shown in Fig. 6. The reactor was maintained at a nominal 2-W power level throughout the experiment to retard the buildup of long-lived fission-product gamma-ray emitters in the core, and the control elements were placed in the outside rows to reduce the perturbation of the flux at the core interior.

---

[10] D. J. Knowles, A Computer for a Position Indicating System, ORNL-2534 (July 18, 1958).

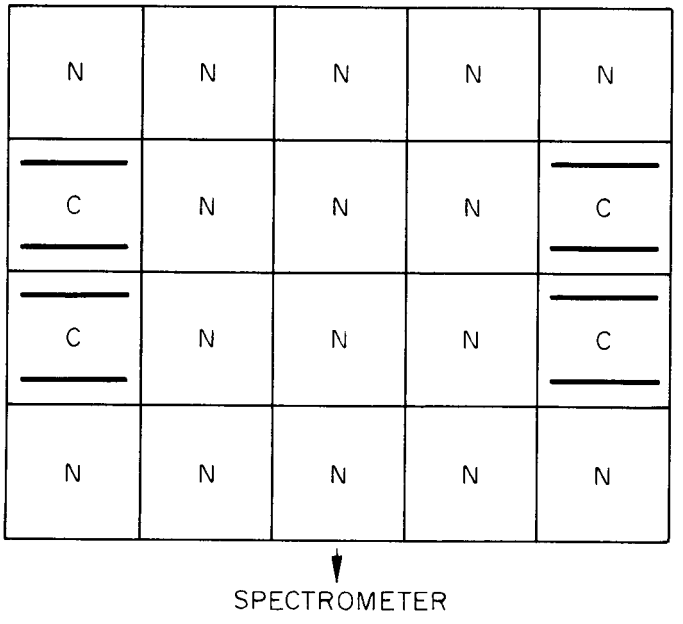

NOTE: SEE ORNL 2470, PAGE 8, FOR DETAILS OF THE ELEMENTS

Fig. 5. Plan View of Reactor Loading During Gamma-Ray Spectral Measurements.

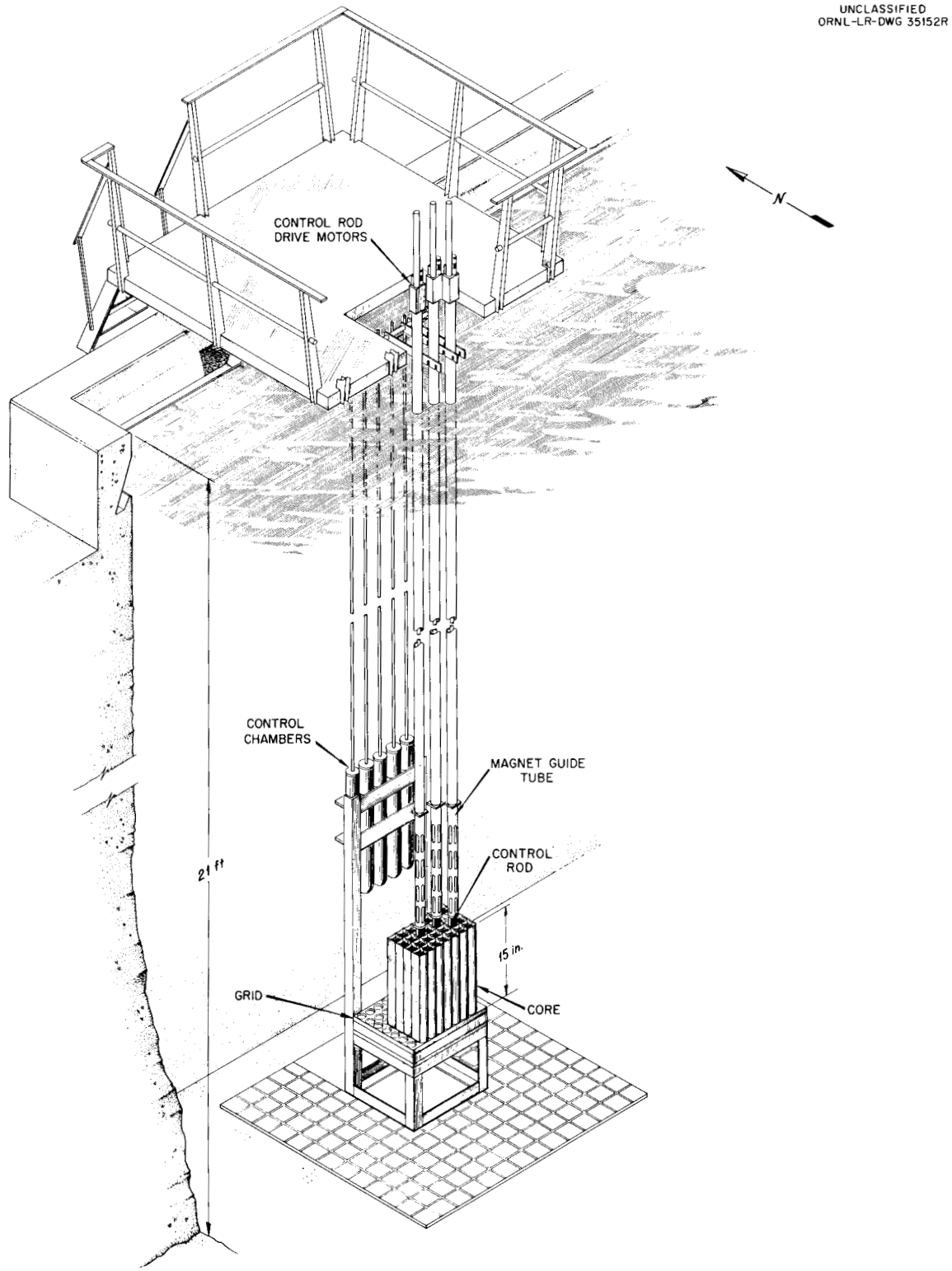

Fig. 6. A Typical PCA Loading.

In addition to the reactor being monitored with the usual reactor control instruments, it was also monitored with external instrumentation as shown in the block diagram in Fig. 7. A 3-in.-diam fission-plate detector located at the east face of the reactor and gold foils exposed in the core during each run were used as neutron monitors. A 50-cc ion chamber located adjacent to the fission-plate detector was used to monitor gamma-ray intensity. The 2-W power level was maintained for a minimum of 1 hr before any gamma-ray data were taken, and the data were taken then only if the ion-chamber reading had become constant, implying an equilibrium gamma-ray condition.

Spectrometer Instrumentation

All instrumentation used for obtaining the spectra, as well as that used for count-rate monitoring during each run, was conventional. Figure 8 shows the interconnections in a block diagram. The power was supplied in parallel to the individual photomultiplier tubes by means of a voltage divider between the tubes and the single 1500-V d-c power supply. The power supply output was monitored by comparing the output across a 1-mA load with the current from a standard cell located in a temperature-insulated box near the power supply. A deviation, which was continually recorded, of less than 1% caused a full-scale (10-mV) deflection on a strip-chart recorder. A deviation of two minor divisions on the chart (0.02%) was considered sufficient cause to terminate a run. The gain of the individual photomultiplier tubes was adjusted by varying the power at the voltage divider until the peak of the pulse-height distribution for the 1.84-MeV gamma ray from ^{88}Y fell in the same channel of the pulse-height analyzer for each tube operating singly. At the beginning of the experiment each tube was checked daily, but when the gain shift due to the individual

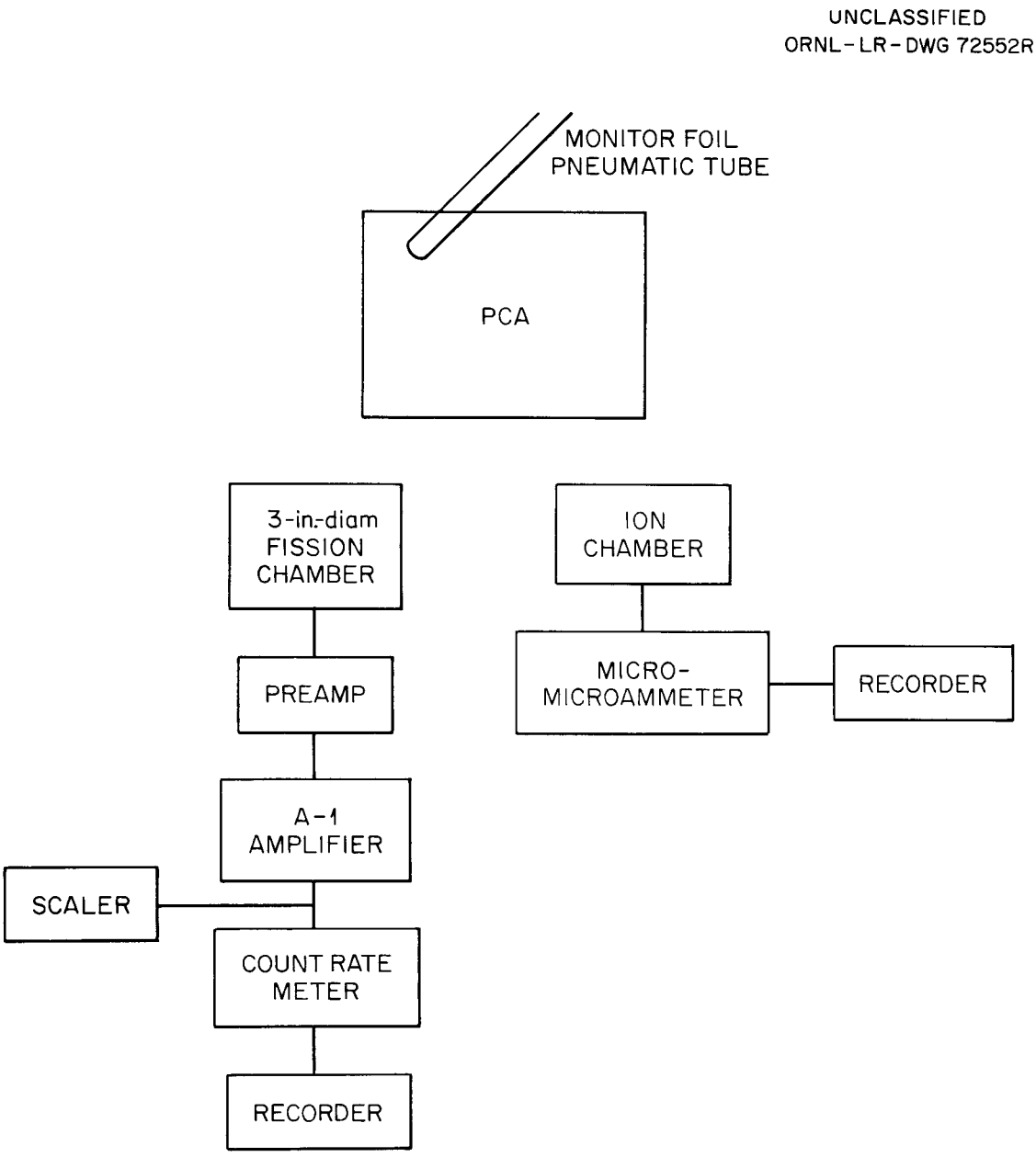

Fig. 7. Block Diagram of Reactor Monitoring System Electronics.

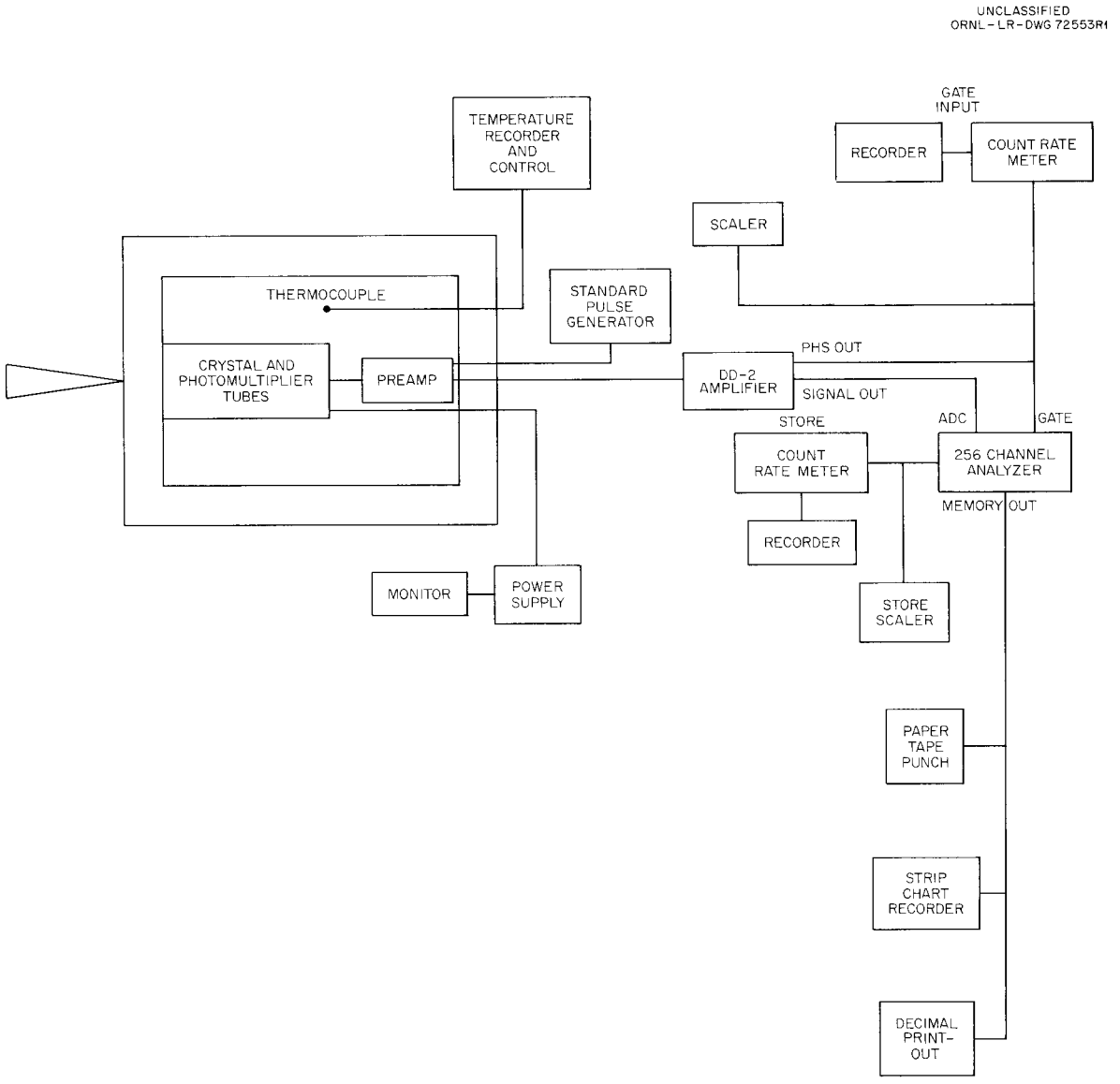

Fig. 8. Block Diagram of Spectrometer Electronics for Measurement of Spectra from a Stainless Steel Reactor Core.

tubes was found to be less than that expected for the whole electronic system (as determined by a standard pulser), the tubes were checked only twice a week.

A cathode-follower circuit located in the spectrometer shield was used to drive the 50 ft of RG 62/U coaxial cable required to transmit the signal to the final amplifier. Final amplification of the signal was obtained with the use of a double-delay-line amplifier (DD-2).[11] The pulses were then transmitted to a 256-channel pulse-height analyzer,[12] where they were stored in a particular channel of a magnetic-core memory, depending on their pulse heights. To prevent random noise pulses from being recorded, the pulse-height-selector (PHS) output signal from the amplifier, which was biased above the amplifier noise, was used to initiate (gate) the analysis and storage process in the analyzer. The rate at which these gate pulses were presented to the analyzer was continuously monitored with a count-rate meter and strip-chart recorder. In addition, the integrated count rate was recorded with a decade scaler for each run. It was discovered that deviations in analyzer power-supply output would cause significant changes in the rate at which all pulses were stored in the analyzer memory. In order to assure that this had not occurred during a run, the stored-pulse frequency was monitored with a system comparable to that used at the analyzer input. The variable dead time of the analyzer was taken into account automatically by means of a live-time circuit[13] designed and built at ORNL. This circuit kept the analyzer operative for a preset live time and then caused it and all monitoring circuits to stop simultaneously.

---

[11] E. Fairstein, Rev. Sci. Instr. 27, 476 (1956).

[12] R. L. Chase, Nuclear Pulse Spectrometry, McGraw-Hill, New York, 1961.

[13] N. W. Hill, Instrumentation and Controls Div. Ann. Progr. Rept. July 1, 1958, ORNL-2647, p 1.

Three methods were used to recover the data from the analyzer: by decimal print-out, strip-chart recorder, and punched-paper tape. The decimal print-out provided a permanent record of the data, with the strip-chart recording providing a rapid inspection of the data as they would appear when plotted. Both served to point out any serious abnormalities that might appear in the data. The punched-paper tape, which was coded in hexadecimal notation, was used as a temporary storage medium prior to the data being converted to punched cards for use with the IBM-7090 computer for processing (see "Data Reduction," below). The last channel of each data tape contained a unique identification number which was eventually read into the computer and used to check that the correct data were being reduced.

CALIBRATION

In order to establish a direct relation between pulse height (channel number) and gamma-ray energy, the spectrometer was calibrated with sources of gamma rays of known energies before and after each run. During any run greater than 4 hr, a calibration was also made near the middle of the run. As an indication of the consistency of the calibrations, the channel expected to correspond to a 7-MeV pulse height was determined from the results of 30 individual calibration runs. It was found to be channel 96.95 ± 0.92, with the extremes of the deviation falling in channels 95.21 and 97.96. Since the 30 values were chosen to be representative of the data acquired during the period of about one year, it was concluded that the channel-to-energy conversion is accurate to within $\pm$ 1%.

The gamma-ray energies used for calibration were 0.899 and 1.840 MeV from ^{88}Y, 0.511 and 1.274 MeV from ^{22}Na, 0.662 MeV from ^{137}Cs, and 0.697, 1.487, and 2.186 MeV from ^{144}Pr (daughter product of ^{144}Ce). These sources

were embedded in the material of the rotatable shutter shown in Fig. 1 and could be used for calibration checks at any time. Higher energy gamma rays were made available by activating ^{23}Na and the demineralized water in the BSR-I.

The water was circulated through the reactor core and then through the front section of the gamma-ray collimator at a flow rate rapid enough for the 6.12-MeV gamma ray emitted during the decay of ^{16}N to be observed. The distribution for this gamma-ray energy is shown in Fig. 2. After each use of this source the collimator was carefully checked to assure that it contained no residual activity.

Small samples of $NaCO_2$ were activated in the reactor to make decay gamma rays from ^{24}Na with energies of 1.368 and 2.754 MeV available as calibration energies. Because neither the ^{24}Na source nor the ^{16}N source could be conveniently used when the spectrometer was under water, their use was restricted to the beginning and end of each day.

A precision pulse generator was used as a secondary standard for calibration during the experiment. Although this method bypassed the crystal and photomultiplier tubes, it did afford a rapid and accurate test of the electronics from the preamplifier through the pulse-height analyzer. Since the statistical spread of the signal from the pulser was much less than the spread of the pulse-height distribution about a given gamma-ray energy and since it was known that the output of the pulser was linear within 1%, the pulser could be expected to give a very accurate indication of any linearity change that might have occurred in the system.

During the experiment it was noticed that an increase in the count rate would cause a sudden change in the apparent gain of the system. This

trouble was found to result from the inability of the analyzer power supply to provide sufficient current for the analog-to-digital converter circuit with the higher count rates -- an effect that has been noticed with at least one other analyzer similar to the one used here. It was found, however, that the gain shift acted as a "step function" and could be adequately corrected for by a numerical redistribution of the measured spectra by using a Fortran II program.[14]

DATA REDUCTION

Reduction of the data for the many measurements made during the experiment was completely automated through the use of the IBM-7090 computer and auxiliary equipment at the Oak Ridge Gaseous Diffusion Plant. Many computational programs were written to reduce the data to the units reported here and to apply corrections as needed. All the programs were written in Fortran II language for compatability with the existing monitor system. Details of those programs that are of more general usefulness are given in another report,[14] and their application during this work is briefly discussed in the following paragraphs.

Two types of pulse-height distributions were taken during the experiment: calibration runs, which were distributions containing peaks indicating the presence of gamma rays with known energies (see "Calibration"), and the distribution of gamma rays emanating from the reactor. Conclusions relative to the observed structure of the reactor gamma-ray distribution would, of course, be dependent on the information gained from the

---

[14] J. D. Jarrard and G. T. Chapman, Some Fortran Codes Used in the Initial Reduction of Data Taken with Multichannel Pulse-Height Analyzers, ORNL-TM-659 (Sept. 16, 1963).

calibration spectra. During this phase of the work the total information required from the calibration distributions was a consistent check on the constancy of the equipment and the best estimate of the relation between pulse-height and gamma-ray energy.

All data for computational purposes were obtained from the pulse-height analyzer on punched-paper tape. The information on the tapes was in hexadecimal notation and had to be converted to cards or magnetic tape to meet computer input requirements. A program written for the CDC-160A was used to transfer the data from the paper tape directly to punched cards, which were subsequently read into the IBM-7090, where the information was then converted to binary-coded decimal through the use of TAPEX, a special program.

After the data were corrected for time and the background was subtracted, it was desired to obtain the best estimate of the most probable channel (pulse height) for a given energy peak in the calibration distributions. A modified form of a general nonlinear least-squares fitting program was used for this purpose. But since at least five parameters were required as input for each estimate, time was saved by writing an auxiliary program, PREPAR, which required only the number of peaks in the distribution and the first and last channels of each peak as input to make the first estimate of the five parameters. PREPAR also provided a deck of punched cards containing all the necessary information for the fitting program.

The fitting program gave as auxiliary information the best estimate of the width of a peak at 1/e<u>e</u>th of the Gaussian fit. Since the same gamma-ray sources were used for calibration throughout the experiment, this number, which is a measure of the crystal resolution, was used to monitor any

changes that might have occurred in the crystal-photomultiplier system.

Finally, the output of the fitting program was subjected to a bivariate-polynomial least-squares fitting program (BIFIT) to obtain the best available pulse-height-to-energy conversion for application to the reactor spectra.

The program was written in sections so as to permit frequent inspection of the data, but each program was required to prepare the input information for the subsequent program. This feature eliminated essentially all the manual key punching required for large programs such as this one.

BACKGROUNDS

Relatively small inherent backgrounds are associated with a large sensitive detector such as the NaI(Tl) crystal used in the Model IV gamma-ray spectrometer. Two experimenters[15] using comparable crystals concluded that the predominant sources of the low-energy rays are in the materials and space surrounding the crystal rather than in the crystal itself. In another study[16] it was shown that gamma-ray peaks up to about 9 MeV may be expected in the backgrounds because of the interaction of cosmic rays in the high-Z materials commonly used as shields around such a crystal.

A detailed analysis of the origin of such background radiations is not germane to this report. We do include, however, the results of a study that was made prior to the reactor spectral measurements to assure that

---

[15] S. Raboy and C. C. Trail, Nucl. Instr. Methods 9, 145-148 (1960).

[16] H. A. May, Radiological Physics Division Semiannual Report January through June, 1962, ANL-6646, p 50.

the background had been reduced to a minimum. These results are plotted in Fig. 9, and the main structure of the distribution is briefly described in the following paragraphs.

The data shown as the open circles in Fig. 9 were taken with the spectrometer in the air above the reactor pool. Any change in the count rate with the shutter open and with it closed was not statistically significant provided that the BSR was not operated at high power while the measurements were made and that the spectrometer was pointed away from the other reactors (the Oak Ridge Research Reactor and Low-Intensity Test Reactor) in the immediate area. The data represented by the closed circles were taken with the spectrometer under about 19 ft of water and about 6 ft away from the surface of the PCA and with the collimator end pointed toward the reactor (the acceptance cone was not used during these measurements). Here, too, the count-rate difference with the reactor operating at a nominal 2 W and with the reactor shut down was statistically insignificant as long as the shutter remained closed. Below about 3.5 MeV the magnitude of the count rate for measurements made in air was essentially the same as for those made in water.

Data Above 3.5 MeV. -- Above 3.5 MeV, pulses were observed all the way to at least 300 MeV, with peaks occurring at about 7 and 116 MeV. Since the distribution was observed to be attenuated by 30% or more when the spectrometer was under water, these pulses were assumed to be due primarily to cosmic-ray interactions in the shield.

When shown the distribution for the measurements made in air, Mather[17] suggested that the distribution at 116 MeV was due to mu-mesons (muons) traversing the crystal with minimum ionization and that the energy deposited in the crystal would be proportional to the path length through the crystal.

---

[17] R. L. Mather, USNRDL, private communication.

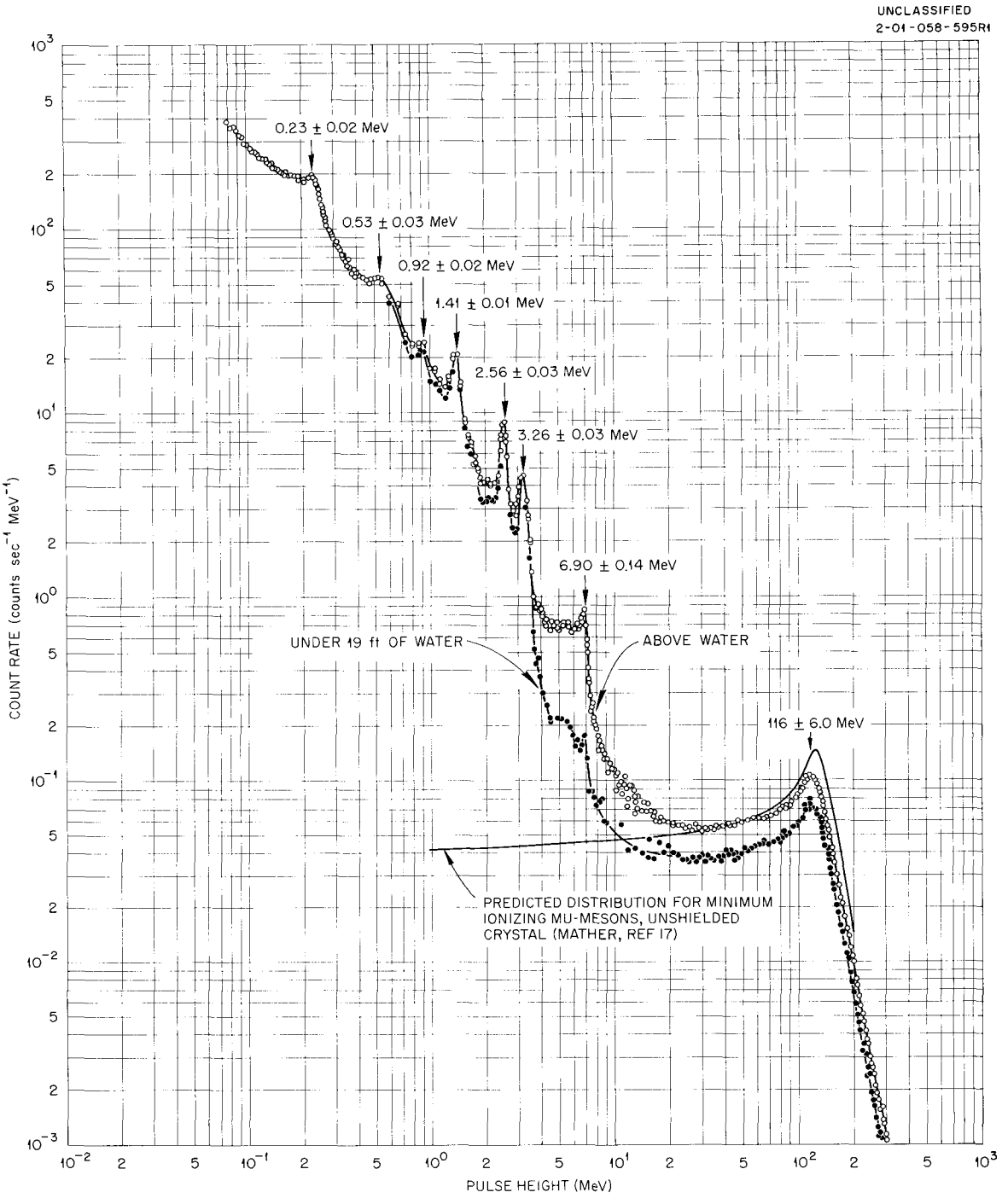

Fig. 9. Background Associated with the Model IV Gamma-Ray Spectrometer.

He then was able to calculate the path-length distribution for a cylindrical crystal geometry similar to that used here based only on "...geometry, stopping power theory, and handbook information on cosmic rays at sea level."[17] The agreement with the measured distribution is most satisfactory, as shown in Fig. 9. The curve is the direct output of the calculations for an unshielded crystal without the benefit of normalization. The peak of the calculated distribution falls at 121 MeV, whereas the measurements reflect a peak at 116 $\pm$ 6.0 MeV.

The peak at 6.9 MeV probably indicates the binding energy in one of the lead isotopes. Measurements[18] of the capture gamma rays of ^{207}Pb and ^{208}Pb indicate that the product nuclei decay directly to the ground state by the emission of 6.734 and 7.380 MeV, respectively. Either of these transitions could be responsible for the 6.9-MeV peak observed, but neutron capture by ^{207}Pb is favored since this isotope contributes[19] about 90% to the lead-capture cross section for thermal neutrons, whereas ^{208}Pb contributes only about 0.18%.

In order to determine whether the other reactors (LITR and ORR) near the spectrometer were responsible for the number of neutrons required to produce the 6.9-MeV photon peak, the spectrometer was oriented at various angles to the reactors and measurements were made at different locations in the building. It appeared that the other reactors were contributing only a small number of the neutrons. Therefore the following complex cosmic-ray interactions were considered as the origin of the neutrons:

---

[18] L. V. Groshev et al., Atlas of γ-Ray Spectra from Radiative Capture of Thermal Neutrons, Pergamon, New York, 1959.

[19] Ibid., p 17.

1. Mu^--mesons may produce neutrons through a capture process comparable to a K electron capture, and there is at least an 80% probability that during the transmission a high-energy x ray (K_α) is emitted which, for lead, has an energy of 6 MeV.[20] In addition, the capture of slow mu^--mesons gives on the average of two neutrons per capture which are emitted in the range 14 to 24 MeV.[21]

2. The high-energy neutrons and protons in cosmic rays at sea level may also produce evaporation neutrons in nuclear interactions which, although much less in number than the mu^--mesons, interact much more readily with matter. Their interaction with lead releases on the average of 6.5 neutrons per interaction.[16]

All the neutrons considered above would have to have been reduced to thermal energy before undergoing the capture process giving rise to the gamma-ray energy mentioned.

As shown in Fig. 9, the 116-MeV peak for measurements made in air was lowered by a factor of about 1.3 when the measurements were made under water, and the 6.9-MeV peak was lowered by a factor of almost 5. This implies that the source of the neutrons was primarily the evaporation neutrons resulting from the interaction of the proton and neutron cosmic-ray components, since these components are more readily attenuated by water. If the neutrons had resulted from mu^--meson capture, a peak representing the 6-MeV K_α x ray would probably have been apparent in the distribution obtained when the spectrometer was in air.

---

[20] H. A. May, Radiological Physics Division Semiannual Report January through June, 1962, ANL-6646, p 51.

[21] R. D. Sard and M. F. Crouch, Prog. Cosmic Ray Phys. 2, 3 (1954), cited in Handbuch der Physik, S. Flugge, Ed., Vol. XL, p 530, Springer, Berlin, 1957.

Data Below 3.5 MeV. -- The pulses measured below 3.5 MeV were believed to be due primarily to gamma rays being emitted during the decay of natural radioisotopes in the lead. Figure 10 is a decay scheme which would explain the observed peaks. The 8 x 10^5-year ^{208}Bi decays to an 8-nsec metastable state by the emission of a 0.92-MeV gamma ray,[22] then to the ground state by the further emission of a 0.51-MeV gamma ray. Subsequently, the ^{208}Bi decays to the 2.615-MeV level of ^{208}Pb (ThD) by 100% electron emission. We would have expected to find both the 0.92- and the 0.51-MeV peak in the distribution rather than the one peak labeled "1.41-MeV." Because the life time of the metastable state is short compared with the time resolution of the crystal, it is possible that the sum of these two energies (1.43 MeV) contributed to the 1.41-MeV peak, although this possibility should be greatly reduced because of geometric consideration. It is more probable that the 1.41-MeV peak is the result of the decay of ^{40}K to the ground state of ^{40}Ar through the 1.46-MeV level of the latter nucleus. The presence of this gamma ray was observed by Raboy and Trail,[15] who were able to show that the ^{40}K was not located in the crystal or photomultiplier tubes and circuitry.

The remaining peaks may be explained through the consideration of the last transition in the ThC (ThC $\xrightarrow{\alpha}$ ThC" $\xrightarrow{\beta}$ ThD) chain.[22,23] The beta decay

---

[22] K. Way et al., Nuclear Data Sheets, vol 5, National Academy of Sciences and National Research Council, 1962.

[23] R. D. Evans, The Atomic Nucleus, Chap. 16, McGraw-Hill, New York, 1955.

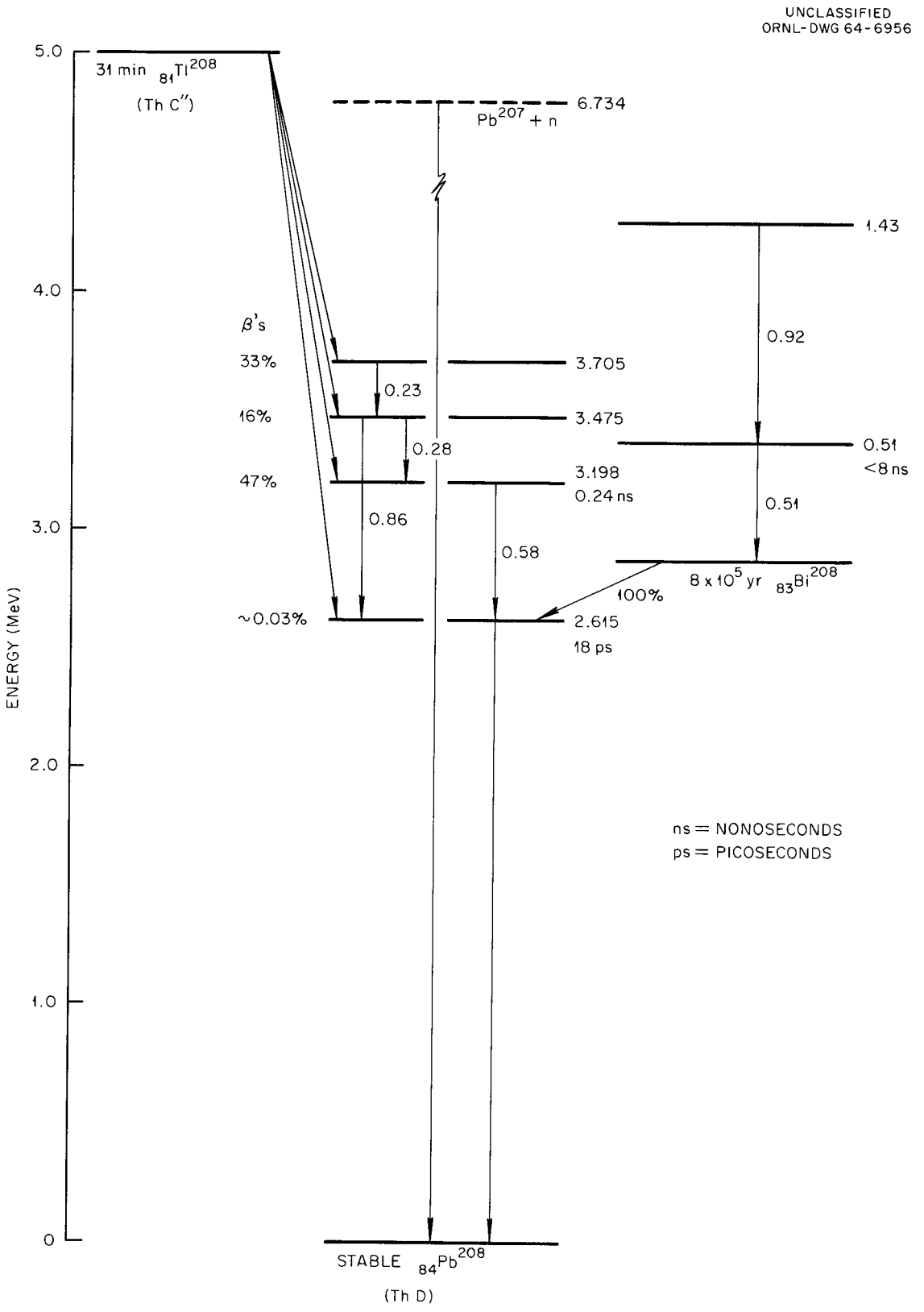

Fig. 10. Decay Scheme Proposed for Explaining the Inherent Background for the Model IV Gamma-Ray Spectrometer.

from the ground state of $^{208}_{81}Tl$ (ThC") feeds four of the ^{208}Pb (ThD) levels with sufficient intensity for the decay from these levels to be observed with the detector. On the average, 33% of the time the decay is to the 3.709-MeV level in ^{208}Pb, which subsequently decays to the 3.475-MeV level by emitting a 0.23-MeV gamma ray. Due to the separation of other peaks in the distribution, it is believed that a peak should be observable even with the resolution of this crystal. Of the other decay paths indicated in Fig. 10, the most significant is that from the 3.198-MeV metastable state through the 2.615-MeV metastable state, which is accomplished by the emission of a 0.583-MeV gamma ray from a heavily populated level to a short-lived level at 2.615 MeV and thus to ground by the further emission of this amount of energy. Here again, we would have expected to find peaks at 0.583 MeV, 2.615 MeV, and their sum (3.198 MeV) for the same reasons as above, assuming that some thorium was present in the crystal and crystal housing. Further, it would have been expected that the peaks at 2.615 and 3.198 MeV, as well as the peak at 1.43 MeV, would be relatively large because of the high probability of excitation of the levels which give rise to these energies. Such is observed in the distribution, and since the errors quoted in Fig. 9 are conservative, there is a good correlation between the measured energies and those expected, as shown in Table 1.

Despite the amount of water between the reactor and the shield at all times, there was an additional continuum in the background of about 10% of the distribution shown in Fig. 9 when the spectrometer was within its closest approach to the reactor.

Table 1. Possible Origin of Background Radiations

Observed Peak (MeV)	Expected Energy (MeV)	Possible Origin
116.00 ± 6.0	121	Minimum ionized mu-meson
6.90 ± 0.14	6.739	$^{207}Pb(n,\gamma)^{208}Pb$
3.26 ± 0.03	3.198	Sum (0.583 + 2.615); ThC" $\xrightarrow{\beta,\gamma}$ ThD
2.56 ± 0.03	2.615	Primarily $^{208}Bi \xrightarrow{\beta,\gamma} {}^{208}Pb$
1.41 ± 0.01	1.46 1.43	Primarily $^{40}K \rightarrow {}^{40}A$ Sum (0.92 + 0.51) ^{208}Bi
0.92 ± 0.02	0.92	Level in ^{208}Bi
0.53 ± 0.03	0.51 and/or 0.583[a]	Levels in ^{208}Pb and/or ^{208}Bi
0.23 ± 0.02	0.23	Level in ^{208}Pb or accumulated Compton backscattering

[a]These two levels could have been smeared in the distribution by the instrument resolution.

PULSE-HEIGHT SPECTRA

The geometry of the experiment relative to the reactor is shown in Fig. 11. All measurements were made in the horizontal plane containing the x and z axes. The distances referred to in this section are for the thickness of water between the surface of the reactor and the entrance to the acceptance cone.

Figure 12 shows the pulse-height spectrum at various distances from the reactor for gamma rays emitted normal to the reactor surface. The data have been corrected for the energy-dependent collimator geometry (see Appendix A) and normalized to a nominal 1-W reactor power. In addition, they have been analytically adjusted[14] to correct for the slight gain shift previously mentioned and for intrinsic efficiency of the crystal. Errors are not indicated on the figure because of the uncertainty in the accuracy of the reactor power. The count-rate statistics in most cases is comparable to the height of the symbol.

It will be noted in Fig. 12 that the spectrum above 5 MeV is predominantly due to gamma rays resulting from the capture of thermal neutrons in the reactor structural material. A few of these gamma-ray energies and the isotopes responsible are indicated on the figure for reference. The peak at about 6 MeV arises from two ^{57}Fe capture gamma rays of almost equal intensity and with energies[18] of 5.914 and 6.015 MeV, respectively. These energies and many others in the measured spectrum are too close together to be completely resolved by the large NaI(Tℓ) crystal used. Another ^{57}Fe capture gamma ray, found at 7.639 MeV, appears as the most distinct peak in the high-energy capture spectrum. The distribution between 8.5 and 9.0 MeV is composed of gamma rays from strongly excited levels in ^{54}Cr at 8.881 MeV

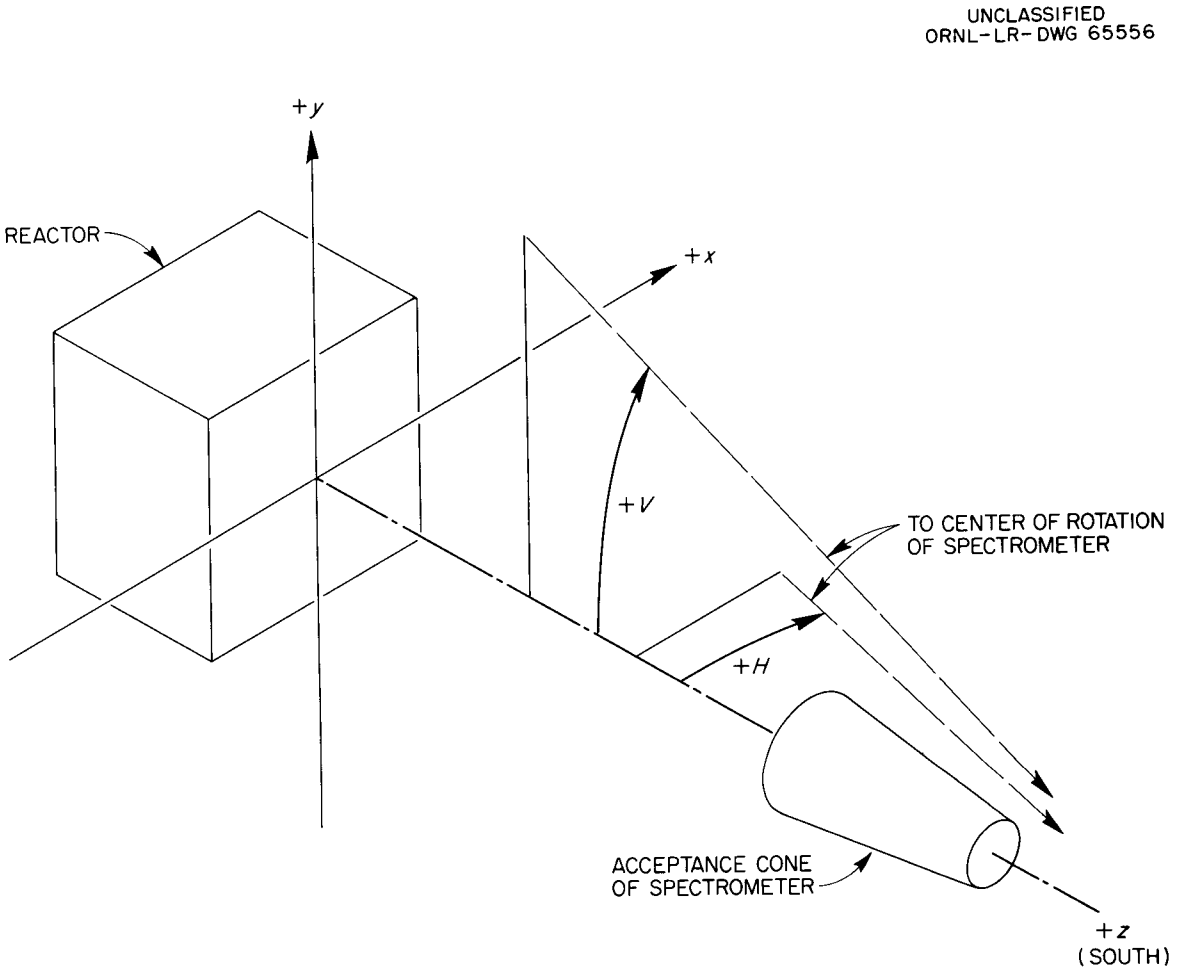

Fig. 11. Geometry for Gamma-Ray Spectral Measurements.

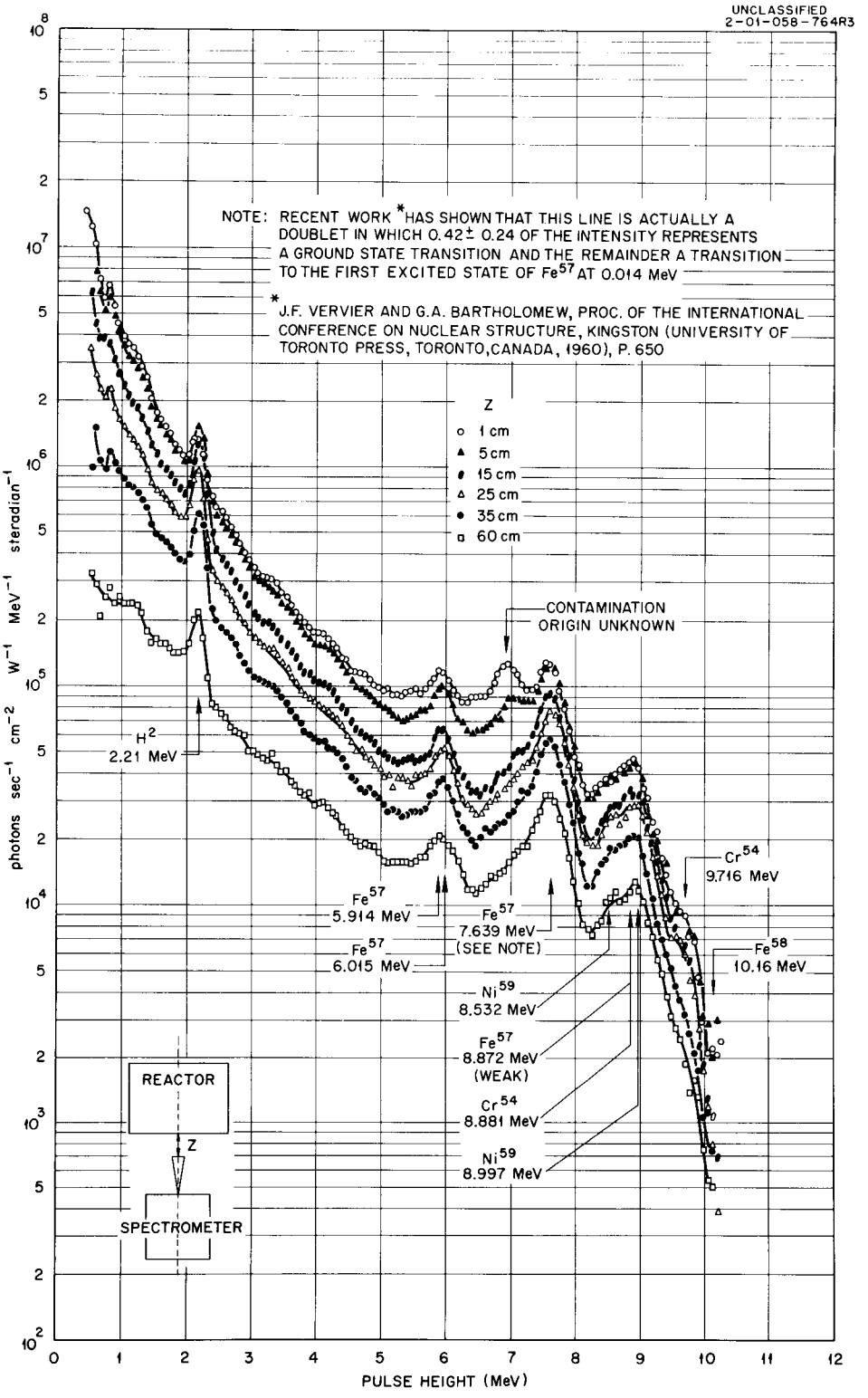

Fig. 12. Pulse-Height Distribution of Gamma Rays Emitted Normal to the Surface of a Stainless Steel Reactor as a Function of the Distance in Water from the Reactor Surface. (The lines are drawn only to indicate the individual sets of data.)

and in ^{59}Ni at 8.532 and 8.997 MeV plus a weak contribution of gamma rays from ^{57}Fe at 8.872 MeV. Above 9 MeV, the major contribution comes from ^{54}Cr at 9.716 MeV and from ^{58}Fe at 10.16 MeV.

Below 5 MeV the spectrum shown in Fig. 12 is apparently composed of gamma rays which constitute the expected continua of prompt-fission and fission-product gamma rays plus the very strong contribution from the 2.22-MeV level excited by thermal-neutron capture in the hydrogen of the water. The data show an intensity maximum for this particular gamma ray at about 5 cm from the reactor surface, which is to be expected, since the number of thermal neutrons available for capture in the water is greatest at about 4 cm from the reactor surface.

A peak in the data at about 6.9 MeV seems to disappear as the spectrometer is moved away from the reactor surface. The origin of this contamination is not yet understood, but appears to be a capture gamma ray associated with some material in the spectrometer shield or cone.

Figures 13 and 14 show the effect on the spectrum as the spectrometer is rotated about points in the water at 10 and 25 cm from the surface of the reactor. At increased angles the hydrogen-capture gamma ray (2.213 MeV) becomes very predominant and shows little attenuation relative to the higher energy portion of the spectrum. This again implies that the origin of these water-capture gamma rays is primarily in the shield-reflector region rather than in the core of the reactor. Other than this relative change in the intensity of the hydrogen-capture gamma ray and with the exception of the 6.9-MeV "contamination" peak discussed above, the general shape of the spectrum remains constant with changes in angle.

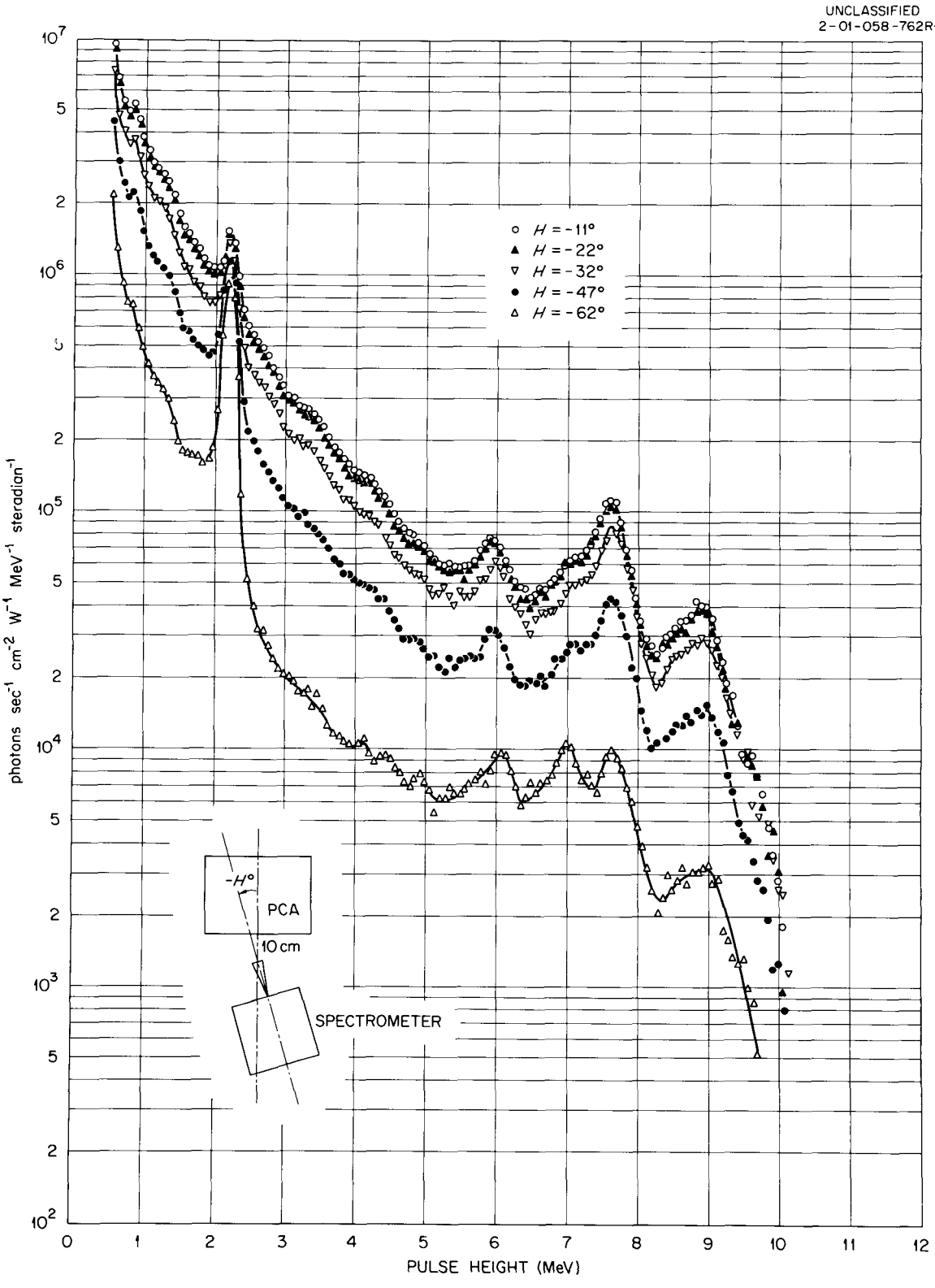

Fig. 13. Pulse-Height Distribution of Gamma Rays as a Function of Angle About a Point in Water 10 cm from the Reactor Surface. (The lines are drawn only to indicate the individual sets of data.)

Fig. 14. Pulse-Height Distribution of Gamma Rays as a Function of Angle About a Point in Water 25 cm from the Reactor Surface. (The lines are drawn only to indicate sets of data.)

Other gamma rays resulting from thermal-neutron capture by the elements contained in stainless steel exist with energies ranging down to very low levels. However, these emitting levels are closely spaced and very numerous below 5 MeV.[24] In addition, the intensities (photons per capture) of gamma rays from these levels are small compared with those of the gamma-ray sources described above which also contribute to the spectrum below 5 MeV. Consequently, because of the close spacing of the levels and limited ability of the crystal to resolve gamma rays having only small separations in energy (as shown by the measured resolution curve of Fig. 3), these lower energy gamma rays are not expected to appear in these data as distinct peaks. Furthermore, this smearing effect, inherent in the crystal response, tends to overemphasize the magnitude of the distributions at lower energies, thus making the spectrum appear somewhat softer than it actually is. A partial unscrambling of the data, which is under way, should correct for these effects to some extent and give a more accurate approximation of the true photon-energy distribution.

Finally, a detailed mapping of the neutron flux in the reactor is expected to give a more accurate estimate of the reactor power. After this phase of the work is completed, it should be possible to present the data more accurately as photons per Watt or photons per fission.

COMPARISON OF MEASURED SPECTRUM WITH CALCULATIONS

A simple calculation was made of the spectrum of gamma rays at the surface of a reactor for comparison with the experimental measurements. The reactor was assumed to be homogeneous, with the distribution of gamma-ray

---

[24] At least 80 emitting levels below 5 MeV in the major components of stainless steel are reported by Groshev *et al.* in ref 18.

"births" being uniform and the gamma rays being emitted isotropically at the point of "birth." For simplicity, it was also assumed that those gamma rays which suffer more than one collision in the attenuating medium of the reactor core are lost in the core. If a gamma ray undergoes a single Compton scattering collision before escaping, it will be emitted with an energy determined by the angle through which it is scattered. This energy will, of course, be less than the original energy. Thus the spectrum at the surface of the core is composed of those gamma rays which have scattered at least once in the core $[\Gamma_s(E)]$ and of those which escape with the original energy $[\Gamma_\mu(E)]$.

The number of gamma rays passing through the surface after having been scattered is

$$\Gamma_s(E_j) = \frac{[1 - P_o(E_i)]\ (\mu_c/\mu_a) \cdot [\alpha_{ij}\ \nu_T(E_i)\ P_o(E_j)\omega}{2\pi\ S\Delta E}\ , \qquad (1)$$

and the number which escapes with the original energy is

$$\Gamma_\mu(E_i) = \frac{P_o(E_i)\ \nu_T(E_i)\omega}{2\pi\ S\Delta E}\ , \qquad (2)$$

where the symbols are defined in Table 2 and the factor 2π is introduced because only those gamma rays emitted outwardly from the reactor core are counted. The probabilities $P_o(E)$ and α_{ij} and the distribution of gamma rays $\nu_T(E)$ are discussed below.

The Average Escape Probability $[P_o(E)]$

The escape probability, averaged over the volume as defined by Case, de Hoffman, and Placzek,[25] is a function only of the attenuating properties of the medium and the geometry of the problem. The following two geometric

[25] K. M. Case, F. de Hoffman, and G. Placzek, Introduction to the Theory of Neutron Diffusion, Vol. I, Chap. II, Los Alamos Scientific Laboratory, Los Alamos, New Mexico, 1953.

Table 2. Symbols and Definitions

E_i	Initial photon energy, MeV
$P_o(E_i)$	The escape probability averaged over the reactor volume, V
$\mu_c(E_i)$	Linear absorption coefficient for Compton scattering for gamma ray(s) with energy E_i in the reactor, cm^{-1}
$\mu_a(E_i)$	Total linear absorption coefficient for gamma ray with energy E_i in the reactor, cm^{-1}
E_j	Energy after scattering of a photon with initial energy E_i
$\nu_T(E_i)$	Energy distribution of gamma rays in the reactor, photons/fission
S	Reactor surface area, cm^2
ΔE	Energy bin width, MeV
ω	3.1×10^{10} fissions sec^{-1} W^{-1}
$\Gamma_\mu(E_i)$	Total photons that leave the surface with their initial energy E_i MeV, photons sec^{-1} cm^{-2} steradian^{-1} W^{-1} MeV^{-1}
$\Gamma_s(E_j)$	Total photons that leave the surface after degradation to energy $E_j \leq E_i$ by virtue of Compton scattering, photons sec^{-1} cm^{-2} steradian^{-1} W^{-1} MeV^{-1}
α_{ij}	Normalized probability that a photon with initial energy E_i will have energy between $E_j - \Delta E$ and E_j after a Compton scattering event
r	Radius of a spherical reactor, cm
t	Thickness of a slab reactor, cm
k	0.511 MeV
r_o	Classical electron radius
σ_o	Thompson classical cross section $=(8/3)\pi r_o^2$
$\gamma(E_i)$	$(3/8)[\sigma_o/\sigma_T(E)]$ (k/E_i^2) MeV^{-1}
σ_T	Total Compton cross section, cm^2

configurations were assumed for bracketing the actual geometry of the reactor core in this calculation:

1. A slab of finite thickness (t), but infinite in the other dimensions:

$$P_o(E) = \frac{1}{t\mu_a}\left[\frac{1}{2} - E_3\,(t\mu_a)\right], \tag{3}$$

where the function $E_3\,(t\mu_a)$ is tabulated in ref 26.

2. A sphere of radius (r):

$$P_o(E) = \frac{3}{8(r\mu_a)^3}\left[2(r\mu_a)^2 - 1 + (1 + 2r\mu_a)\,e^{-2r\mu_a}\right]. \tag{4}$$

The Scattering Probability (α_{ik})

The differential cross section for the scattering of a photon of initial energy E_i into the energy interval E to E + ΔE is[27]

$$\frac{d\sigma(E_i)}{dE} = \frac{\pi\, r_o^2 k}{E_i^2}\left[\frac{E}{E_i} + \frac{E_i}{E} - 2\left(\frac{k}{E} - \frac{k}{E_i}\right) + \left(\frac{k}{E} - \frac{k}{E_i}\right)^2\right], \tag{5}$$

with the condition that $E_i \geq E \geq \dfrac{E_i}{1 + \dfrac{2E_i}{k}}$. The probability[28] that the

---

[26] D. K. Trubey, A Table of Three Exponential Integrals, ORNL-2750 (June 18, 1959).

[27] A. T. Nelms, Graphs of the Compton Energy - Angle Relationship and the Klein-Nishina Formula from 10 KeV to 500 MeV, NBS Circular 542 (1953).

[28] G. de Saussure, A Calculation of the Gamma-Ray Spectrum of the Bulk Shielding Reactor, ORNL CF-57-7-105 (July 31, 1957).

photon will be scattered into the energy interval E_{j-1} to E_j is[29]

$$\eta_{ij} = \frac{1}{\sigma_T(E_i)} \int_{E_{j-1}}^{E_j} \frac{d\sigma(E_i)}{dE}\, dE , \qquad j \le i. \tag{6}$$

Upon substituting Eq. (5) into (6) and performing the integration, we have

$$\eta_{ij} = \gamma(E_i) \left[\frac{1}{2E_i} (E_j^2 - E_{j-1}^2) + \left(E_i - 2k - \frac{2k^2}{E_i}\right) \ell n \left(\frac{E_{j-1}}{E_j}\right) \right.$$

$$\left. + \left(\frac{2K}{E_i} + \frac{k^2}{E_i^2}\right) (E_j - E_{j-1}) - k^2 \left(\frac{1}{E_j} - \frac{1}{E_{j-1}}\right) \right] , \tag{7}$$

where $\gamma(E_i) = \frac{3}{8} \frac{\sigma_o}{\sigma_T(E_i)} \frac{k}{E_i^2}$ MeV^{-1} and the normalized probability becomes

$$\alpha_{ij} = \frac{\eta_{ij}}{\sum_{j=1}^{i} \eta_{ij}} . \tag{8}$$

For the calculation presented here, all energy bins are constant so that

$$\Delta E = E_j - E_{j-1} = 0.5 \text{ MeV} \tag{9}$$

and the expression for η_{ij} becomes

$$\eta_{ij} = \gamma(E_i) \left[\frac{\Delta E}{2E_i} (2E_j - \Delta E) + \left(E_i - 2k - \frac{2k^2}{E_i}\right) \ell n \left(\frac{E_j - \Delta E}{E_j}\right) \right.$$

$$\left. + \left(\frac{2k}{E_i} + \frac{k^2}{E_i^2}\right) \Delta E + \frac{k^2\, \Delta E}{E_j (E_j - \Delta E)} \right] . \tag{10}$$

---

[29] Since a gamma ray may have any energy $E_j \le E_i$ after a scattering event, the upper edge of each energy bin will be set equal to E_i (or E_j) so that the integration allows a given gamma ray to scatter "down" into its own bin. This may be thought of as "small-angle scattering."

The calculated probabilities (α_{ik}) are given in Table 3.

The Input Spectra (ν_T)

With one exception, all input spectra were taken from published experimental data. Gamma rays originating from the following processes were considered as contributing to the source spectra:

1. neutron capture in the atoms of the stainless steel constituents,[30]
2. neutron capture in hydrogen,[30]
3. prompt fission,[31]
4. fission-product gamma-ray emitters,[32]
5. neutron captures in ^{235}U.

A search of the literature failed to produce any measured spectra of the gamma rays resulting from neutron capture in ^{235}U; so the approximation used was one proposed by de Saussure,[28] namely, that the energy spectrum up to the binding energy of an additional neutron has the same shape as the prompt fission spectrum. This is probably not a bad approximation for this calculation since these gamma rays contribute little to the total number of source photons at the higher energies.

The stainless steel was assumed to consist of only the five major components Fe, Ni, Cr, Si, and Mn. Since the intensities were given as photons per 100 captures, the average number of photons per fission falling in the

---

[30] L. V. Groshev et al., "Atlas of γ-Ray Spectra from Radiative Capture of Thermal Neutrons," in International Series of Monographs on Nuclear Energy (R. A. Charpie and J. V. Dunworth, eds.) (translated by J. B. Sykes), Pergamon, New York, 1959.

[31] F. C. Maienschein, private communication.

[32] R. W. Peelle, W. Zobel, and T. A. Love, Appl. Nuclear Phys. Div. Ann. Progr. Rept., September 10, 1956, ORNL-2081, p. 94.

Table 3. Probability of Compton Scattering from Initial Energy Group E_i into Final Energy Group E_j
(Energy values represent the upper edge of a 1/2-MeV-wide group)

Initial Photon Energy E_i (MeV)	Compton Scattering Probability For E_j =																			
	1.0 MeV	1.5 MeV	2.0 MeV	2.5 MeV	3.0 MeV	3.5 MeV	4.0 MeV	4.5 MeV	5.0 MeV	5.5 MeV	6.0 MeV	6.5 MeV	7.0 MeV	7.5 MeV	8.0 MeV	8.5 MeV	9.0 MeV	9.5 MeV	10.0 MeV	10.5 MeV
1.0	1.0000																			
1.5	0.6846	0.3154																		
2.0	0.5746	0.2130	0.2124																	
2.5	0.5167	0.1709	0.1561	0.1562																
3.0	0.4943	0.1537	0.1170	0.1160	0.1190															
3.5	0.4530	0.1360	0.1115	0.1019	0.0987	0.0988														
4.0	0.4327	0.1273	0.1010	0.0995	0.0843	0.0825	0.0825													
4.5	0.4165	0.1211	0.0939	0.0812	0.0748	0.0717	0.0704	0.0705												
5.0	0.4030	0.1163	0.0886	0.0752	0.0680	0.0641	0.0621	0.0613	0.0613											
5.5	0.3916	0.1125	0.0846	0.0708	0.0631	0.0586	0.0560	0.0546	0.0540	0.0540										
6.0	0.3818	0.1094	0.0815	0.0674	0.0593	0.0544	0.0514	0.0496	0.0486	0.0482	0.0482									
6.5	0.3732	0.1068	0.0789	0.0647	0.0564	0.0512	0.0479	0.0458	0.0445	0.0437	0.0434	0.0434								
7.0	0.3655	0.1046	0.0768	0.0624	0.0540	0.0486	0.0451	0.0428	0.0412	0.0402	0.0397	0.0394	0.0395							
7.5	0.3589	0.1027	0.0759	0.0606	0.0521	0.0466	0.0429	0.0404	0.0386	0.0369	0.0367	0.0363	0.0361	0.0361						
8.0	0.3526	0.1009	0.0734	0.0590	0.0504	0.0448	0.0410	0.0384	0.0365	0.0352	0.0343	0.0337	0.0334	0.0332	0.0332					
8.5	0.3470	0.0994	0.0720	0.0577	0.0490	0.0434	0.0395	0.0367	0.0347	0.0333	0.0323	0.0316	0.0311	0.0308	0.0307	0.0307				
9.0	0.3420	0.0980	0.0708	0.0565	0.0478	0.0421	0.0382	0.0353	0.0332	0.0317	0.0306	0.0298	0.0292	0.0289	0.0287	0.0286	0.0286			
9.5	0.3371	0.0967	0.0698	0.0555	0.0468	0.0410	0.0370	0.0341	0.0320	0.0304	0.0292	0.0283	0.0277	0.0272	0.0269	0.0267	0.0269	0.0267		
10.0	0.3325	0.0962	0.0693	0.0550	0.0462	0.0404	0.0363	0.0333	0.0311	0.0295	0.0282	0.0272	0.0265	0.0260	0.0256	0.0254	0.0252	0.0252	0.0252	
10.5	0.3290	0.0945	0.0679	0.0537	0.0450	0.0393	0.0352	0.0322	0.0300	0.0283	0.0270	0.0260	0.0252	0.0246	0.0242	0.0239	0.0237	0.0236	0.0235	0.0234

ith energy group was

$$\nu_c^{SS}(E_i) = \frac{\Sigma_a^{SS}}{\Sigma_f}\left(\frac{1}{100\,\bar{E}_i}\sum_{k=1}^{5}\sum_{j=1}^{n}\frac{\Sigma_a^k}{\Sigma_a^{SS}}E_{jk}\,\lambda_{jk}\right);\ (E_j - \Delta E) \le E_{jk} \le E_i \quad (11)$$

The contribution from hydrogen capture was obtained in a similar manner. It was necessary only to convert the published data for the other spectra to histograms and take the sum for the total intensity. Thus, for a given energy E_i,

$$\nu_T = \nu_c^{SS} + \nu_c^{H} + \nu_{FP} + \nu_P + \nu_c^{25} \quad , \quad (12)$$

where

ν_T = total photons per fission with energy E_i,

ν_c^{SS}, ν_c^{H}, ν_c^{25} = capture photons from stainless steel, hydrogen, and uranium,

ν_{FP} = fission-product photons,

ν_P = prompt-fission photons.

These input spectra are shown in Fig. 15.

Conclusion

The experimental data are compared in Fig. 16 with the calculated spectrum for the assumed spherical and infinite-slab reactor configurations. The gamma-ray attenuation coefficients were taken from APEX-628[33] and NBS Circular 583.[34] It is felt that the close agreement in count rate is fortuitous, since many assumptions were made which would tend to underestimate the spectrum at low energies. Then, too, the calculation represents

---

[33] M. A. Capo, Gamma Ray Absorption Coefficients for Elements and Mixtures, APEX-628 (August 1961).

[34] G. Grodstein, X-ray Attenuation Coefficients from 10 KeV to 100 MeV, NBS Circular 583 (1957).

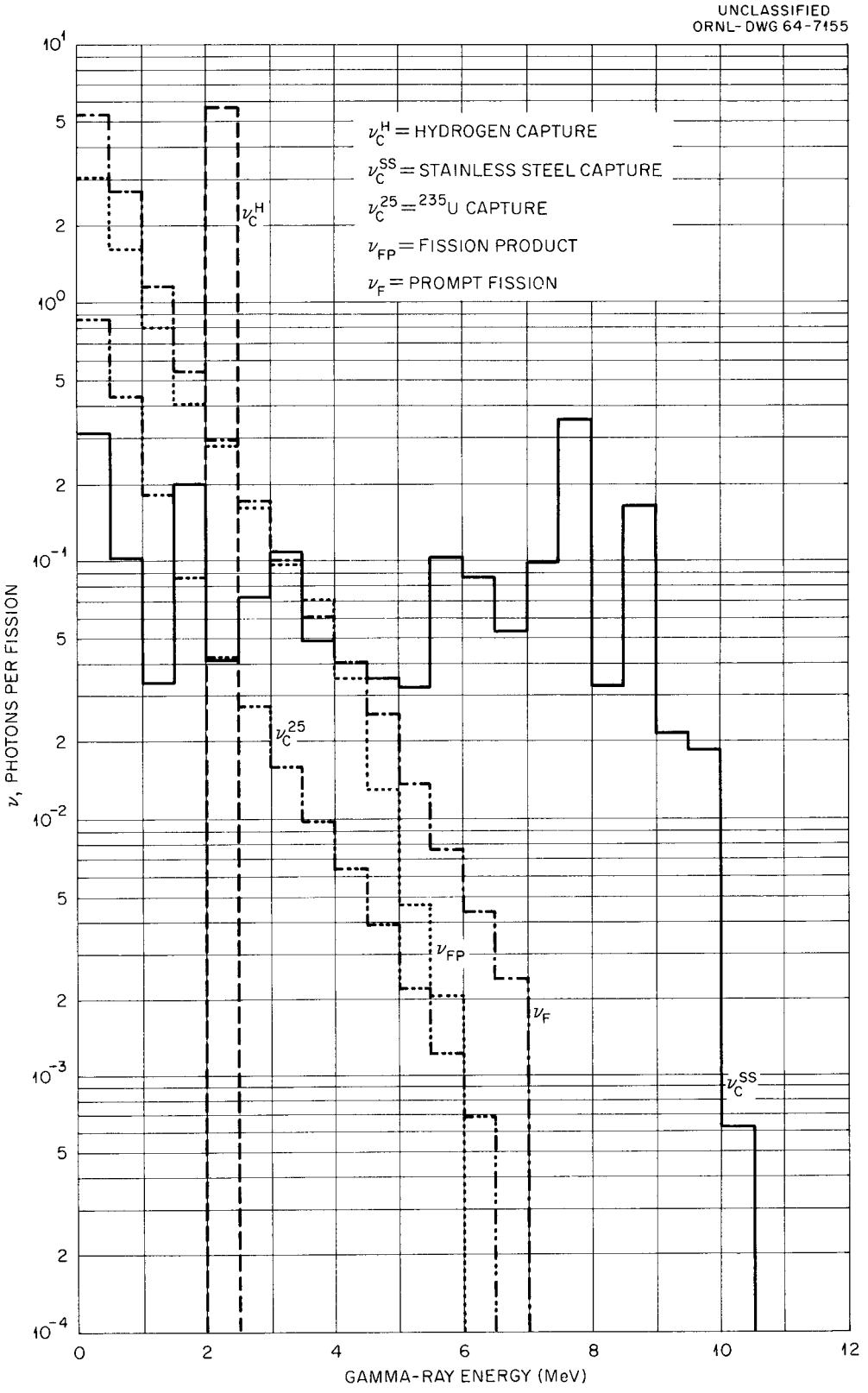

Fig. 15. Gamma-Ray Input Spectra.

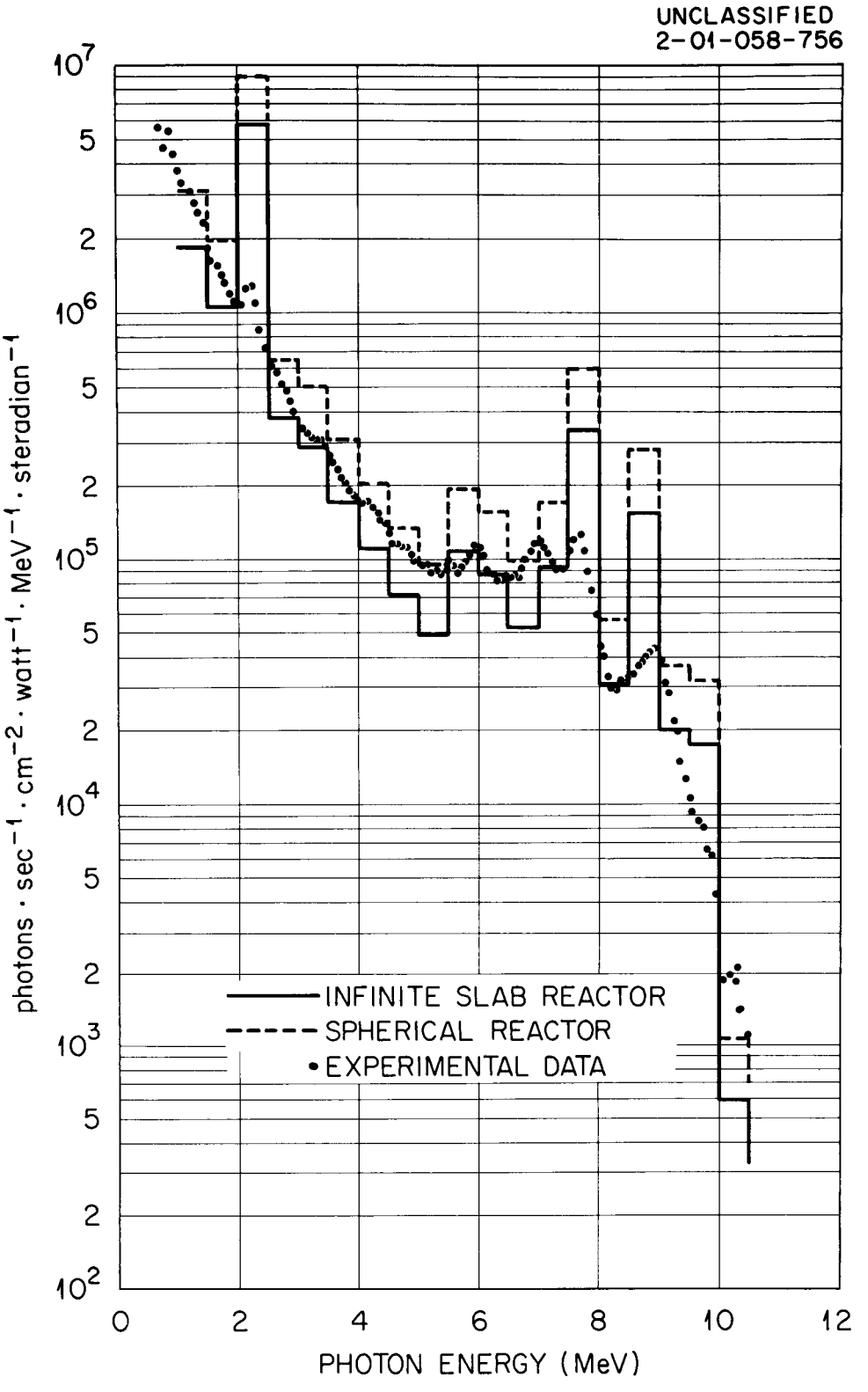

Fig. 16. Calculated Gamma-Ray Spectra Compared with the Measured Spectrum 1 cm from the Reactor Surface and Normal to It.

the spectrum that would be obtained with a "100% peak-to-total, constant resolution spectrometer."[35] This would tend to overemphasize the height of the peaks, as indeed it does. However, the peak-to-total ratio for the spectrometer used is about 50%; so it is not surprising that the calculated peaks are much more predominant than the measured peaks. The calculated peak near 2 MeV, on the other hand, seems to be much too high. No explanation for this can be given at present.

ACKNOWLEDGMENTS

The authors wish to acknowledge with grateful thanks the many periods of discussion and consultation held with F. C. Maienschein, R. W. Peelle, and W. Zobel, the work done by R. L. Cowperthwaite, who originated and wrote much of the first programs used in the data reduction, the cooperative assistance of the staff of the Bulk Shielding Facility during the period in which the data were taken, and the assistance of the many people contacted at the ORGDP Central Data Processing when help was needed on minor problems in coding and communicating with the IBM-7090 computer.

---

[35] The ratio of the area under the peak to the total area under the pulse-height distribution and the percent resolution (full width at half maximum of a gamma-ray peak divided by the gamma-ray energy) are measures of the efficiency of the crystal detector for distinguishing monoenergetic gamma rays.

APPENDIX A

COLLIMATOR CORRECTIONS

When measuring a gamma-ray spectrum with a system in which the photons are collimated through a shield, it is essential to have some estimate of the effectiveness of the collimator in order to correctly evaluate the data. Since no shielding material is absolutely opaque to gamma rays, gamma rays will penetrate small thicknesses of the material at the entrance and exit apertures, even when the shield is thick enough to stop them, effectively increasing the solid angle of the collimator and giving rise to an apparent error in the measured count rate. In addition, gamma rays may be scattered by the collimator walls before reaching the detector. Since scattering degrades the energy of the gamma rays, a disproportionate number of counts may then appear in the "tail" of the measured pulse-height distribution which could be misinterpreted as a reduced efficiency (defined as the ratio of the area under the total absorption peak to the total area of the distribution for monoenergetic photons) for the crystal.

Neither of the above effects is easy to measure with precision. Therefore one must rely on intuition, experience, and the available computations in order to get a reasonable approximation for the required data corrections. Mather[36] investigated the problem analytically, and various experimenters[37-39] have obtained results which apparently substantiate his conclusions. A less sophisticated method, which is based on a curve published by Mather,[40] has

---

[36] R. L. Mather, J. Appl. Phys. 28, 1200 (1957).

[37] F. M. Tamnovic and R. L. Mather, J. Appl. Phys. 28, 1208 (1957).

[38] R. A. Hefferlin and W. E. Kreger, Nucl. Instr. 3, 149 (1958).

[39] L. C. Thompson, Nucl. Instr. Methods 9, 175 (1960).

[40] R. L. Mather, J. Appl. Phys. 28, Fig. 9 (1957).

has been used to obtain an approximation for the collimator response of the Model IV gamma-ray spectrometer used to measure the gamma-ray spectrum of the stainless steel reactor.

The primary difference between the method used for the stainless steel reactor measurement and the method presented by Mather lies in interpretation. Mather suggests that to a first approximation the effect of penetration is the same as that of reducing the collimator length by 1 mean free path of the collimator material at each end (and consequently by implication the same as reducing the shield thickness); in the interpretation presented here approximately the same results are obtained by a slight energy-dependent increase in the radii at the entrance and exit apertures of the collimator and no reduction of the collimator length. It is believed that this interpretation affords a simpler method for calculating the collimator response than that described by Mather.[36]

Figure A.1 shows a shield containing a collimation hole with a geometric radius of r cm. Gamma rays from the point source at P are required to pass through the unobstructed opening before being seen by the detector. If the collimator is assumed to be "optical," the gamma rays which pass through the double-cross-hatched area are the only ones that will be seen when P is displaced from the collimator center line by an amount $x > r$, since all other gamma rays will intercept a surface of the collimator. If $d\sigma$ is an element of this illuminated area, the solid angle subtended by the area $A(z,x)$ is

$$\omega(z,x) = \int_{A(z,x)} \frac{\vec{n}\cdot\vec{\ell}_\sigma}{|\ell_\sigma|} \frac{d_\sigma}{\ell_\sigma^2}, \quad x \geq r, \tag{A.1}$$

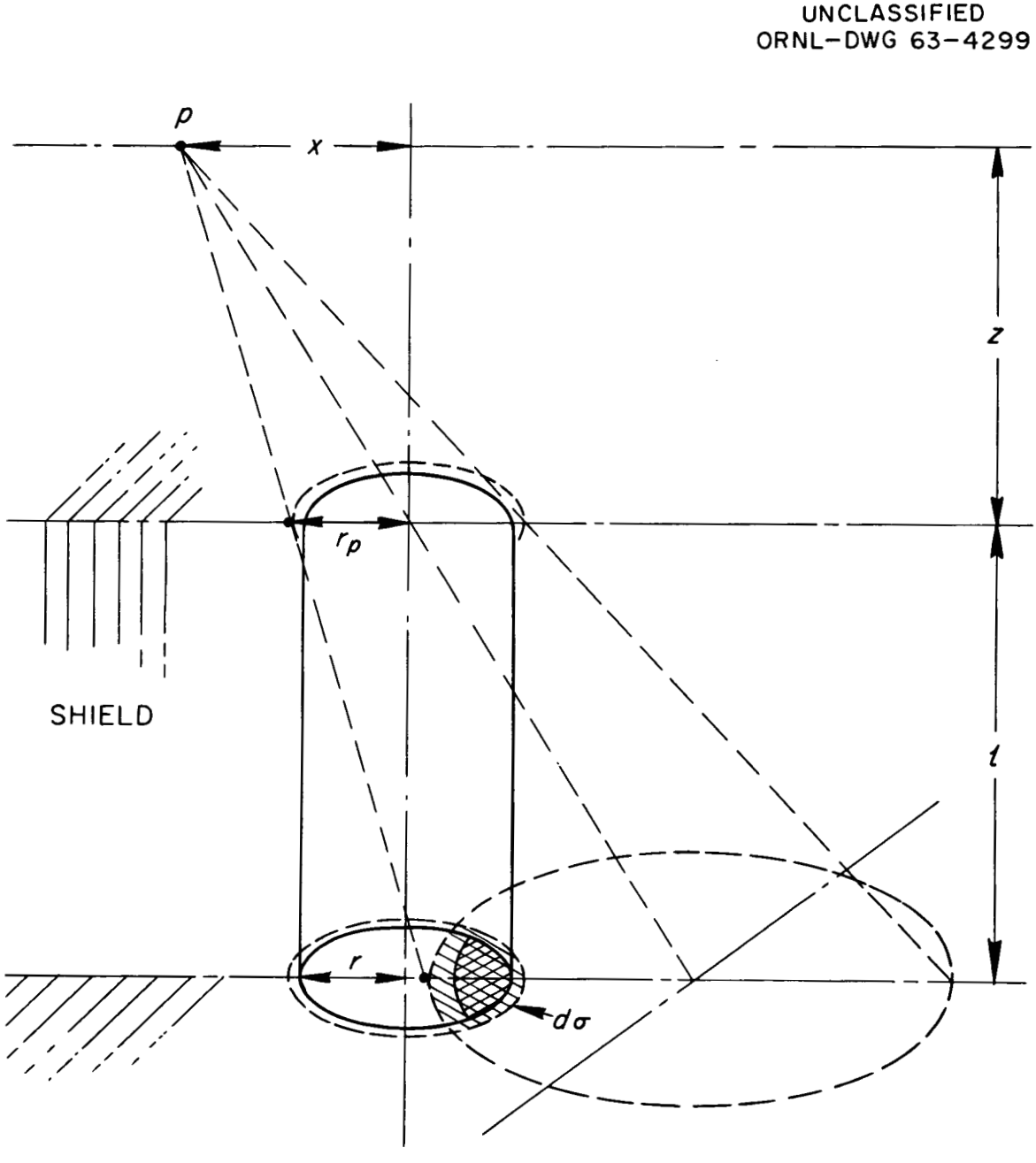

Fig. A.1. Conceptual Change in the Collimator Geometry Due to Penetrating Radiation. Note a slight beveling at the ends. The double cross-hatched area represents the illuminated area due to a point isotropic source of nonpenetrating (optical) radiation. The single cross-hatched area represents the additional illuminated area due to penetrating radiation.

where $\vec{n} \equiv$ a unit vector normal to $d\sigma$ and pointing away from the source, and $\ell_\sigma = \ell_\sigma(z,x)$ = distance from P to $d\sigma$. If the length of the collimator is large compared with the radius, then $\ell_\sigma \cong \ell_s$, where ℓ_s is the distance from the source to the center of the illuminated area $A(z,x)$, and $\vec{n}\cdot\vec{\ell}_\sigma \cong \ell_s \cos\theta \cong \ell_s$. Therefore

$$\omega(z,x) \cong \frac{1}{\ell_s^2} \int_{A(z,x)} d\sigma = \frac{A(z,x)}{\ell_s^2} \quad . \tag{A.2}$$

The illuminated area $A(z,x)$ is simply defined by the intersection of the collimator opening at the exit and the projection of the entrance opening on the same plane. Thus it is obvious that

$$A(z, x \leq r) = \pi r^2 \ , \tag{A.3}$$

and it may be shown that

$$A(z, x > r) = \frac{\pi}{2} r^2(1 + \beta^2) - (\beta - 1)\beta x r(1 - f_1^2)^{\frac{1}{2}} - r^2(\beta^2 \phi_1 + \phi_2), \tag{A.4}$$

where

$$\beta = 1 - \frac{\ell}{z} \ ,$$

$$f_1 \equiv \frac{(\beta - 1)x^2 + (\beta + 1)r^2}{2\beta r x} \ ,$$

$$\phi_1 \equiv \text{arc sin } f_1,$$

$$\phi_2 \equiv \text{arc sin} \left[\frac{(\beta - 1)x^2 - (\beta + 1)r^2}{2rx} \right] ,$$

and r, x, ℓ, and z are defined in Fig. A.2.

If, however, the gamma rays are allowed to penetrate the edges of the collimator, the radius at each end of the collimator hole is assumed to be increased to r_p cm, as shown by the dashed lines of Fig. A.1. The amount

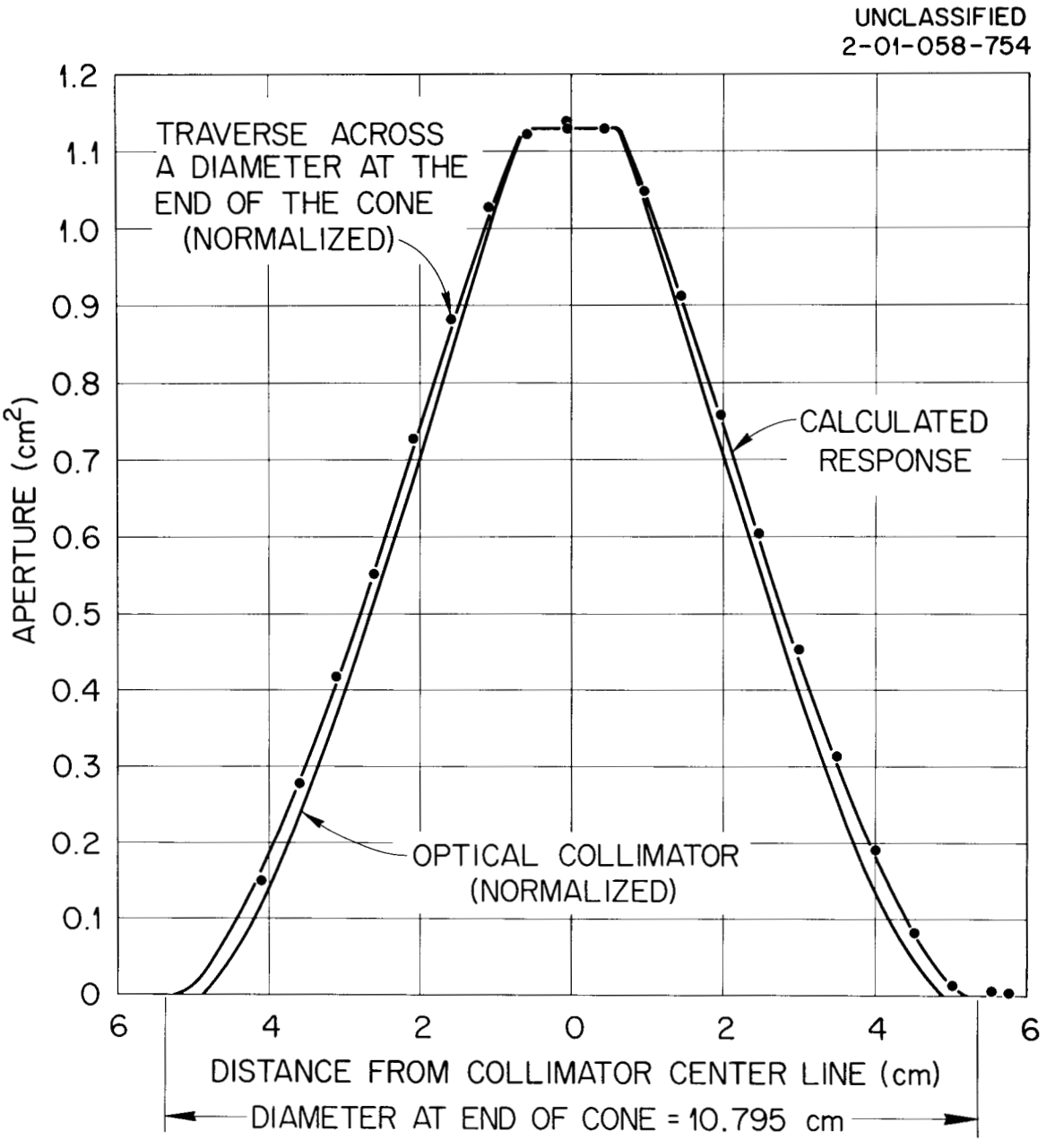

Fig. A.2. Collimator Response for 0.662-MeV Gamma Rays.

of the energy-dependent increase is derived from Fig. 9 of Mather's paper,[40] in which the ratio of the penetration area to the geometric area is given vs the collimator length in mean free paths of material. It will then be noticed that the illuminated area is increased by the amount shown with the single cross hatching. Substituting the new energy-dependent radius into Eq. (A.4), an estimate of the solid angle for a given gamma-ray energy may be obtained from

$$\omega(z,x,E) = \frac{A(z,x,E)}{\ell_s^2} \quad . \tag{A.5}$$

Figure A.2 shows A(z,x,E) for 0.662-MeV gamma rays plotted against source location as the source was moved away from the collimator axis. The dimensions and materials of the collimator used in the calculations corresponded to those of the Model IV spectrometer, and the source was assumed to be at a distance z equal to the length of the spectrometer cone. The integrated count rate as a function of position x obtained by moving a small source of 0.662-MeV gamma rays (^{137}Cs) diametrically across the end of the cone is shown normalized to the calculated value at the collimator center line. The agreement is obvious, even with the effects of scattering neglected in the calculation. The normalized response for an "optical" collimator is shown on the same figure to emphasize the error that may exist if penetration is not considered.

ORNL-3609
UC-34 — Physics
TID-4500 (34th ed.)

INTERNAL DISTRIBUTION

1. Biology Library
2-4. Central Research Library
5. Reactor Division Library
6-7. ORNL — Y-12 Technical Library Document Reference Section
8-57. Laboratory Records Department
58. Laboratory Records, ORNL R.C.
59. E. P. Blizard
60. G. T. Chapman
61. K. M. Henry
62. L. B. Holland
63. J. D. Jarrard
64. E. B. Johnson
65. W. H. Jordan
66. C. E. Larson
67. F. C. Maienschein
68. J. M. Miller
69. R. Peelle
70. D. P. Roux
71. R. T. Santoro
72. M. J. Skinner
73. J. A. Swartout
74. D. K. Trubey
75. J. W. Wachter
76. A. M. Weinberg
77. R. C. Weir
78. R. A. Charpie (consultant)
79. G. Dessauer (consultant)
80. M. L. Goldberger (consultant)
81. R. F. Taschek (consultant)

EXTERNAL DISTRIBUTION

82. Matt Barrett, Nuclear Utility Services, 1730 M Street, Washington, D.C.
83. A. B. Chilton, 264 Mechanical Engineering Building, University of Illinois, Urbana, Illinois
84. Radiation Research Associates, Inc., 1506 W. Terrell, Fort Worth, Texas 76104
85. Pierre LaFore, Commissariat a L Energie Atomique, Centre D'Etudes Nucleaires, de Fontenay-Aux-Roses, Boite Postale No. 6, Seine, France
86. A. M. Saruis, Centro Di Calcolo, CNEN, Via Mazzimi 2, Bologna, Italy
87. B. V. Bhanot, Physics Department, Panjab University, Chandigarh-3, India
88. Research and Development Division, AEC, ORO
89-733. Given distribution as shown in TID-4500 (34th ed.) under Physics category (75 copies — CFSTI)